ectopic expression of *Hmgn2* by electroporation, Hmgn2 is shown to antagonize erythroid differentiation of erythroleukaemia cells and mouse FL cells *in vitro*.

2. Materials and methods

2.1. Animals and cell lines

C57BL6J mice were purchased from Nihon SLC (Hamamatsu). Noon on the day of the plug was defined as 0.5 dpc (day post coitum). To analyse their cells, pregnant mice were killed and their embryos dissected out. Animals were handled according to the Guidelines for the Care and Use of Laboratory Animals of Kyushu University. This study was approved by Animal Care and Use Committee, Kyushu University (Approval ID: A21-068-0). The Friend erythroleukaemia cell line, F5-5.fl, was purchased from the RIKEN Bio-Resource Center. Cells were maintained in RPMI 1640 (Wako Pure Chemical Industries) containing 10% FBS (fetal bovine serum) and 10 units/ml penicillin and 10 mg/ml streptomycin (Sigma–Aldrich). Cells were passaged every 3–4 days.

2.2. Construction of an *Hmgn2* vector

A primer set was designed from the known mouse mRNA sequence (accession no. NM_016957). Full-length *Hmgn2* was amplified from mouse FL cDNA and ligated into the pIRES2-AcGFP (*Aequorea coerulescens* green fluorescent protein) vector (Clontech). *Hmgn2* was located upstream of an IRES (internal ribosome entry site), which was flanked downstream by cDNA encoding AcGFP (Supplementary Figure S2B available at http://www.cellbiolint.org/cbi/036/cbi0360195add.htm). *Hmgn2* sequence was confirmed by DNA sequencing. Endotoxin-free plasmid was prepared using the QIAGEN® Plasmid Midi kit (QIAGEN). The construct was introduced into $CaCl_2$-competent DH5α *Escherichia coli* by the heat shock method.

2.3. Preparation of FL MNCs (mononuclear cells)

At 12.5 dpc, embryonic blood cells were collected by disassociating FL on a 40 μm nylon mesh and washed once with PBS. MNCs were obtained after centrifugation with lympholyte solution (CEDARLANE Laboratories). MNCs were washed twice in PBS and cultured for 24 h in α-MEM (α-minimum essential medium) containing 10% FBS, 20 ng/ml each of SCF (stem cell factor) and TPO (thrombopoietin) (PEPROTECH) and 10 units/ml penicillin and 10 mg/ml streptomycin (Sigma–Aldrich). Floating cells were used for electroporation.

2.4. Electroporation and cell differentiation

Friend erythroleukaemia cells were collected after 24 h culture and washed twice with PBS. Cells were resuspended in Gene Pulser® electroporation buffer (Bio-Rad) at 5×10^6 cells/ml. The cell suspension (400 μl) was mixed with 8 μg of endotoxin-free pIRES2-*Hmgn2-AcGFP* or pIRES2-*AcGFP* (mock), transferred into an electroporation cuvette (0.4 cm gap) and placed on ice for 5 min. Cells were electroporated using a Gene Pulser MXCell™ Electroporator (Bio-Rad) at optimized conditions (200 volts, 2000 μF, 1000 Ω and 20 ms). They were cultured in RPMI 1640 containing 10% FBS without antibiotics for 48 h. GFP (green fluorescent protein)-expressing cells were collected using a FACS Aria cell sorter (BD Biosciences) and cultured in RPMI 1640 containing 10% FBS, 10 units/ml penicillin and 10 mg/ml streptomycin (Sigma–Aldrich) for 6 days.

For FL MNCs, cells were collected by gently pipetting and washing twice with PBS. Cells were electroporated as above. Optimal conditions for FL cells were 300 volts, 2000 μF, 1000 Ω and 20 ms. Cells were cultured with α-MEM containing 10% FBS, 20 ng/ml each of SCF and TPO (PEPROTECH) without antibiotics for 48 h. GFP^+ $CD71^+$/$Ter119^-$ cells were collected using a FACS Aria cell sorter (BD Biosciences) and cultured in α-MEM containing 10% FBS, 20 ng/ml each of SCF, IL-3 (interleukin 3) and EPO (erythropoietin) (PEPROTECH) with 10 units/ml penicillin and 10 mg/ml streptomycin.

2.5. Flow cytometry and cell sorting

To isolate HSCs and erythroid cells, cells were stained with a FITC-conjugated anti-mouse CD71 antibody (BD Biosciences), a PE (phycoerythrin)-conjugated anti-mouse Sca-1 (stem cell antigen-1) antibody (BD Biosciences), an APC (antigen-presenting cell)-conjugated anti-mouse c-Kit (CD117) antibody (BD Biosciences), a PE-Cy7-conjugated anti-mouse CD45 antibody (eBioscience) and an APC-Cy7-conjugated anti-mouse Ter119 antibody (eBioscience) (Hattangadi et al., 2010; Inoue et al., 2011). To analyse differentiation of erythroleukaemia and erythroid cells from FL, cells were stained with an APC-conjugated anti-mouse c-Kit (CD117) antibody (BD Biosciences), a PE-conjugated anti-mouse CD71 antibody (eBiosciences), and an APC-Cy7-conjugated anti-mouse Ter119 antibody (eBioscience). Dead cells were excluded by PI (propidium iodide) staining (Life Technologies). Cells were sorted in using a FACS Aria cell sorter (BD). Data files were analysed with FlowJo software (Tree Star Inc.).

2.6. Real-time PCR

RNA was extracted from sorted cells using RNAqueous-4PCR™ and RiboPure™ kits (Life Technologies). mRNA was reverse-transcribed using a high-capacity RNA-to-cDNA kit (Life Technologies). The quality of cDNA synthesis was checked by amplifying mouse β-actin by PCR. Thirty thermal cycles were as follows: denaturation at 95°C for 10 s, annealing at 60°C for 20 s and extension at 72°C for 20 s. Gene expression levels were evaluated using RT–PCR (reverse transcription–PCR) with a TaqMan® Gene Expression Master Mix and StepOnePlus™ RT–PCR machine (Life Technologies). All probes were from TaqMan® Gene Expression Assays (Life Technologies). Samples were taken in triplicate. mRNA levels were normalized to β-actin and the RQ (relative quantity) of expression was compared with a reference sample. Statistical comparisons of RQ values were calculated using a *t* test.

2.7. Antibody staining and confocal microscopy

HSCs and erythroid cells were isolated from FL at 12.5 dpc by flow cytometry as above. They were cytocentrifuged on to glass slides (Matsunami) using a Shandon Cytospin® 3 cytocentrifuge (Thermo Electron Corporation) at 450 rev./min for 7 min. After drying at 25°C, cells were fixed in 1% PFA (paraformaldehyde) in PBS at 4°C for 30 min and washed in PBS 3 times. After blocking with 1% BSA in PBS, cells were stained with a rabbit anti-mouse Hmgn2 polyclonal antibody (Chemicon International) overnight at 4°C. After three washes in PBS, cells were stained with Alexa Fluor® 488 goat anti-rabbit IgG (1:300) (Life Technologies) and TOTO®-3 iodide (642/660, Life Technologies). Samples were examined under a FV-1000 laser scanning confocal microscope (Olympus).

2.8. WB (Western blot) analysis

Protein was extracted from the sorted cells by using Qproteome® Mammalian Protein Prep Kit (Qiagen) and was quantified by using Quick Start™ Bradford Dye Reagent (Bio-Rad Laboratories). Then 5 μg of protein was run on 15% SDS-polyacrylamide gels concurrently with a pre-stained protein marker (Precision Plus Protein™ Standards, Bio-Rad Laboratories) using Laemmli buffer. Gels were trans-blotted on to a PVDF membrane (Immobilon®-P Transfer Membrane, Millipore Billerica). The PVDF membrane was blocked in 5% non-fat dried skimmed milk powder in TBS-T (TBS containing 0.1% Tween-20) at 25°C for 1 h, washed with TBS-T and reacted with 1:1000 rabbit anti-mouse Hmgn2 polyclonal antibody (Chemicon International) overnight at 4°C. The membrane was thoroughly washed and incubated in a solution of 1:1000 goat anti-rabbit IgG-HRP (horseradish peroxidase) conjugate (R&D Systems) at 25°C for 1 h. After washing, signals were visualized by soaking the membrane in substrate solution (Amersham™ ECL® Plus Western Blotting Detection System, GE Healthcare). Images were captured using ChemiDoc XRS (Bio-Rad Laboratories) and data were analysed by Quantity One ver. 4.6.7 (Bio-Rad Laboratories) and displayed as intensity per mm^2.

2.9. Cell cycle analysis

Cells were washed twice with PBS containing 2% FBS and resuspended in 300 μl PBS. They were permeabilized by adding 700 μl 100% ethanol pre-cooled to −20°C. After mixing by gentle inversion, the cell suspension was placed on ice overnight. Cells were collected by centrifugation at 4000 rev./min at 4°C for 2 min. To eliminate RNA, cells were incubated with 50 μl RNase A solution (100 μg/ml) at 37°C for 30 min. To stain DNA, cells were resuspended in 450 μl of staining solution containing 2 μg/ml PI (propidium iodide) in 100 mM Tris/HCl, pH 7.5, 150 mM NaCl, 1 mM $CaCl_2$, 0.5 mM $MgCl_2$ and 0.1% Nonidet P40, and incubated at 25°C for 30 min in the dark. Cells were analysed using a FACS Aria cell sorter (BD Biosciences). The percentages of cells in G_0+G_1 and in S+G_2 phases were calculated using the Watson Pragmatic method and FlowJo software.

2.10. Mitotic analysis by flow cytometry

Mitotic cell status was analysed as per Taylor (2004). Briefly, cells were washed twice in PBS, fixed in 70% ethanol at −20°C and resuspended in 400 μl PBS. Then 1 ml of cold ethanol (pre-cooled to −20°C) was added to the cell suspension, while gently vortexing the ethanol. The cells were fixed for at least 1 h at −20°C, transferred to a 1.5 ml Eppendorf tube and centrifuged at 3800 rev./min at 4°C for 7 min. After removal of supernatant by aspiration, the cell pellet was resuspended with 1 ml of PBS, centrifuged at 3800 rev./min at 4°C for 7 min, and the supernatant removed as above. The cell pellet was resuspended with 1.4 ml of PBS+0.25% Triton X-100 and incubated on ice for 15 min before being centrifuged at 3800 rev./min at 4°C for 7 min before the supernatant was removed. The cell pellet was resuspended in 100 μl 1% PBSBA (BSA in PBS) containing rabbit anti-phosphorylated histone H3 Ser^{10} IgG (Abcam) and incubated for 2 h at 25°C. Tubes were rocked gently for entire period. Then 1.3 ml of PBSBA was added, mixed by inverting and centrifuged at 3800 rev./min at 4°C for 7 min. After removal of the supernatant, the cell pellet was resuspended in 100 μl PBSBA containing Alexa Fluor® 647 goat anti-rabbit IgG (1:200) (Life Technologies) and incubated for 30 min at 25°C in the dark with gentle mixing as above. The cell suspension was washed once with 1.3 ml of PBSBA and centrifuged at 3800 rev./min at 4°C for 7 min. The cell pellet was resuspended in 500 μl of PBS containing 100 μg/ml DNase-free RNase A and incubated at 37°C for 30 min. After cooling on ice for a few seconds, 100 μl PI solution was added and incubated on ice for 15 min in the dark. Cells were analysed by flow cytometry.

2.11. Statistics

Student's *t* test in Microsoft Office Excel 2007 program was used to test a statistically significant differences ($P<0.05$) in the data.

3. Results

3.1. Expression of Hmgn2 in mouse FL during erythroid differentiation

Erythroid cell populations ranging from uncommitted HSCs to mature erythrocytes were sorted by flow cytometry from mouse FL at 12.5 dpc based on expression of the cell surface molecules CD45 (common leucocyte antigen), Sca-1, c-Kit (CD117, stem cell factor receptor), CD71 (transferrin receptor) and Ter119 (glycophorin) (Supplementary Figure S1A available at http://www.cellbiolint.org/cbi/036/cbi0360195add.htm). Erythroid cell populations were identified as follows: (i) the $CD45^+$/$Sca\text{-}1^+$/$c\text{-}Kit^+$ fraction defined HSCs; (ii) the $Sca\text{-}1^-$/$c\text{-}Kit^+$/$CD71^-$/$Ter119^-$ fraction defined BFU-E (burst-forming unit-erythroid); (iii) the $Sca\text{-}1^-$/$c\text{-}Kit^+$/$CD71^+$/$Ter119^-$ fraction defined committed erythroid progenitors or CFU-E (colony-forming unit-erythroid); (iv) the $Sca\text{-}1^-$/$c\text{-}Kit^-$/$CD71^+$/$Ter119^+$ fraction defined pro-erythroblasts; and (v) the $Sca\text{-}1^-$/

c-Kit$^-$/CD71$^-$/Ter119$^+$ fraction defined reticulocytes and erythrocytes (Supplementary Figures S1A and S1B).

To quantify *Hmgn2* expression levels during erythroid differentiation, RT–PCR analysis was carried out on each sorted population. *Hmgn2* expression levels increased slightly as HSCs differentiated into BFU-E (~1.4-fold, Figure 1A), but gradually decreased at later stages of erythroid cell differentiation (Figure 1A). *Hmgn2* expression in BFU-E and CFU-E was 14- and 12-fold higher than in mature erythrocytes, respectively ($P<0.05$; Figure 1A). Examining the expression of Hmgn2 protein by immunohistochemistry, single cell suspensions of HSCs, BFU-E, CFU-E, proerythroblasts and erythrocytes at 12.5 dpc were prepared, spun on to slides, stained with antibody to Hmgn2 and observed by confocal microscopy. Hmgn2 protein was expressed in all fractions (Figure 1B). To quantify the amount of Hmgn2 protein in each faction, WB analysis was used after loading the same amount of protein. Compatible with the immunohistochemistry data, Hmgn2 protein was detected in all fractions, the highest expression level being in the BFU-E fraction (Figure 1C).

3.2. Hmgn2 expression antagonizes erythroleukaemia cell differentiation

To investigate the function of Hmgn2 in erythroid differentiation, *Hmgn2* was ectopically expressed in Friend erythroleukaemia cells. Full-length mouse *Hmgn2* was cloned into an expression plasmid. The deduced amino acid sequence of Hmgn2 indicated 2 NLSs (nuclear localization signals; NLS1 and NLS2) in addition to the NBD and CHUD (Supplementary Figure S2A). Friend erythroleukaemia cells were transfected with plasmids with and without (mock) *Hmgn2* cDNA by electroporation. Two days later, expression levels of *Gata1* and *Klf1* that encode erythroid transcription factors were measured in transfected cells, identified by their GFP staining. Expression of *Gata1* and *Klf1* decreased in GFP$^+$ *Hmgn2*-transfected cells compared with mock controls ($P<0.05$; Figure 2A). However, expression levels of both *Gata1* and *Klf1* did not differ significantly between *Hmgn2*-transfected and mock control cells at day 8 of culture ($P>0.05$; Figure 2A). By flow-cytometry, 69% c-Kit$^+$/CD71$^+$ cells (equivalent to CFU-E) and 4.2% c-Kit$^+$/CD71$^-$ cells (equivalent to BFU-E) were observed in mock controls at day 8 of culture, whereas 21% c-Kit$^+$/CD71$^+$ cells and 12.6% c-Kit$^+$/CD71$^-$ cells were observed in *Hmgn2*-transfected cells, suggesting that ectopic expression of *Hmgn2* suppressed erythroid differentiation (Figure 2B). Moreover, the percentage of CD71$^+$/Ter119$^+$ cells (equivalent to proerythroblasts) in *Hmgn2*-transfected cells was lower than that seen in mock controls (0.16% versus 1.4%; Figure 2B). Thus ectopic expression of *Hmgn2* inhibited erythroid differentiation of Friend erythroleukaemia cells.

3.3. Hmgn2 misexpression increases the number of erythroleukaemia cells at S-phase of the cell cycle

To investigate how Hmgn2 regulates differentiation of Friend erythroleukaemia cells, the cell cycle status of *Hmgn2*-transfected

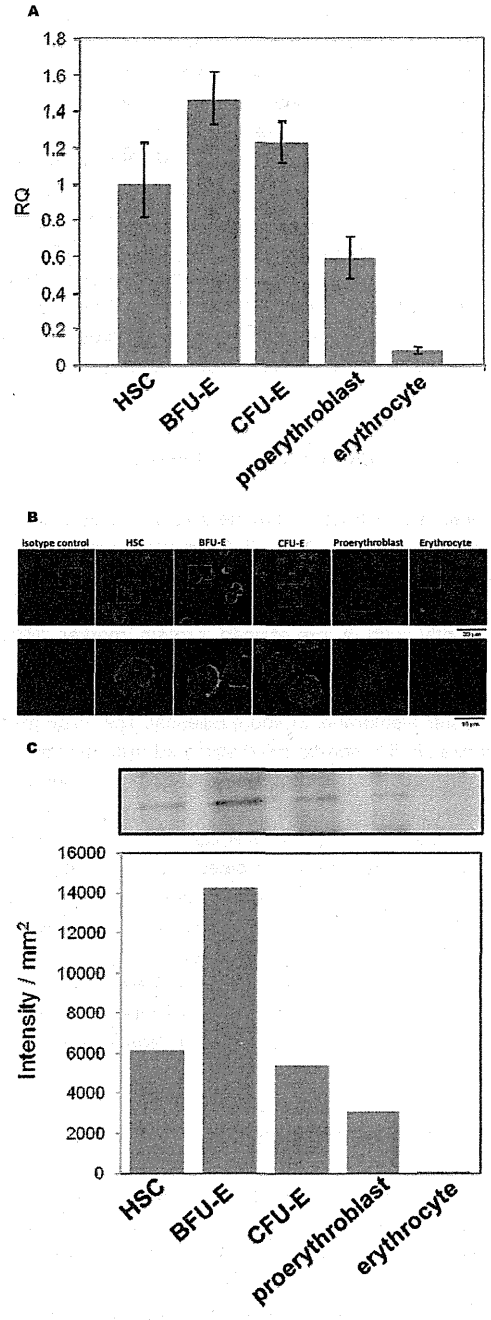

Figure 1 Expression of *Hmgn2* during erythrocyte differentiation in mouse FL
(**A**) Expression of *Hmgn2* in each population of erythroid cells described in Supplementary Figures S1(A) and S1(B) was quantified by RT–PCR. The *y*-axis represents the RQ of gene expression after normalization with β-actin. (**B**) Confocal images of HSCs, BFU-E, CFU-E, proerythroblasts and erythrocytes expressing Hmgn2. Single cells were prepared from mouse FL at 12.5 dpc. Hmgn2 (green) and TOTO®-3 (blue) are shown. Lower panel shows higher magnification of the cells in boxes of upper panel. Scale bars in upper and lower panels indicate 30 and 10 μm respectively. (**C**) WB analysis of Hmgn2 protein in HSCs, BFU-E, CFU-E, proerythroblasts and erythrocytes. Equal amount of protein was trans-blotted on to PVDF membrane and reacted with anti-Hmgn2 antibody. Intensity of protein bands was quantified by Quantity One ver. 4.6.7 and displayed as intensity per mm^2.

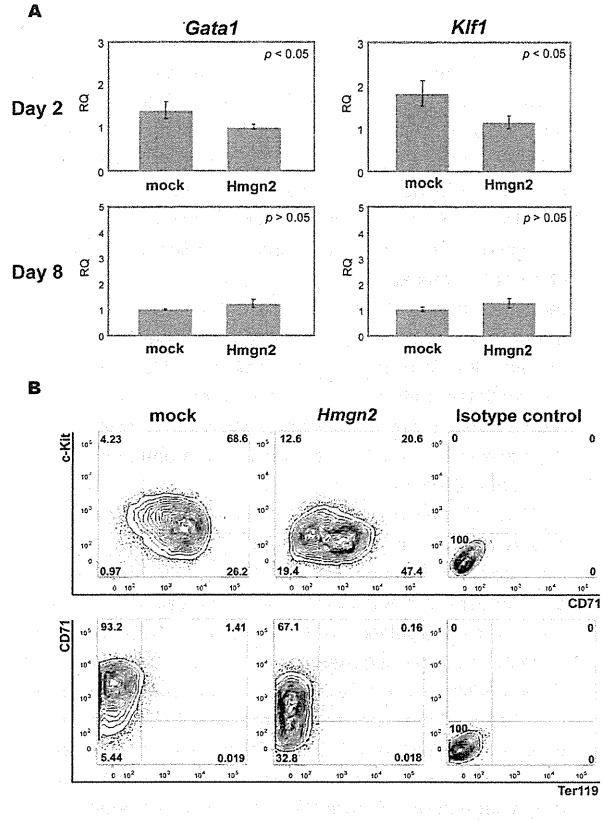

Figure 2 Ectopic expression of *Hmgn2* alters phenotypes of Friend erythroleukaemia cells

(**A**) Expression of transcription factor genes *Gata1* and *Klf1* that regulate erythroid cell differentiation. Gene expression levels in GFP$^+$ cells were quantified by real-time PCR. The *y*-axis represents the RQ of gene expression after normalization with β-actin. Two days after electroporation, *Gata1* and *Klf1* levels in *Hmgn2*-transfected cells were down-regulated ($P<0.05$) (see Supplementary Figure S2C for experimental design). We observed no significant difference in level of *Gata1* and *Klf1* at day 8 of culture ($P>0.05$). (**B**) Flow cytometric analysis for surface markers of Friend erythroleukaemia cells. Surface markers of *Hmgn2*-transfected cells were analysed at day 8 of culture. The percentage of the c-Kit$^+$/CD71$^+$ population in *Hmgn2*-transfected cells (20.6%) was decreased compared with that seen in mock controls (68.6%), whereas the percentage of the c-Kit$^+$/CD71$^-$ population in *Hmgn2*-transfected cells (12.6%) was higher than that seen in mock-transfected cells (4.23%).

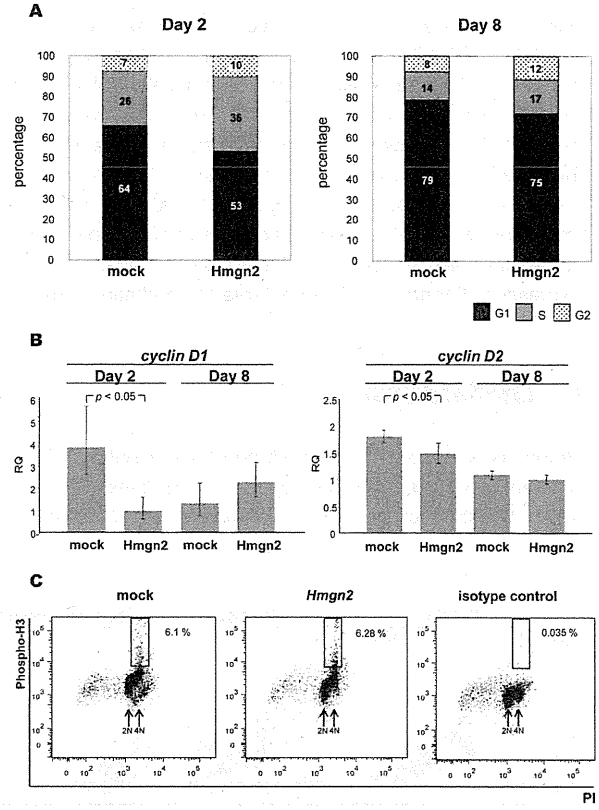

Figure 3 *Hmgn2* misexpression increases in the number of S-phase cells and down-regulates G_1-specific genes

(**A**) The percentage of cells in G_1, S and G_2 phases. Sorted GFP$^+$ cells at day 2 of culture and all cells at day 8 of culture were fixed and stained with PI. DNA content was quantified by flow cytometry. The Watson Pragmatic method was used to calculate cell percentages. (**B**) Expression of the G_1 phase-specific genes *cyclin D1* and *cyclin D2*. Gene expression was measured at days 2 and 8 of culture. The *y*-axis represents the RQ of gene expression after normalization with β-actin. (**C**) The percentage of mitotic status of *Hmgn2*-transfected cells. Sorted GFP$^+$ cells at day 2 of culture were fixed and stained with anti-phosphorylated histone H3 at Ser^{10} (phospho-H3) and PI (DNA content). Mitotic cells were defined as the cells that have 4N content of DNA and high level of histone H3 phosphorylation.

cells by flow cytometry was analysed, with evaluation of expression levels of the G_1 phase-specific genes, *cyclin D1* and *cyclin D2*. Two days after transfection with Friend erythroleukaemia cells with *Hmgn2*, 36% of GFP$^+$ cells were in S-phase, whereas 26% of mock controls were in S-phase ($P<0.05$; Figure 3A and Supplementary Figure S3 available at http://www.cellbiolint.org/cbi/036/cbi0360195add.htm). There was no significant difference in the percentage of cells in S-phase at day 8 of culture between *Hmgn2*-transfected and mock control cells (14 and 17%, respectively, $P>0.05$; Figure 3A). Two days after transfection, expression levels of both *cyclin D1* and *cyclin D2* assessed by real-time PCR were down-regulated in *Hmgn2*-transfected cells ($P<0.05$; Figure 3B). At day 8 of culture, there was no difference in expression levels of *cyclin D1* and *cyclin D2* between *Hmgn2*-transfected and mock control cells (Figure 3B).

To investigate mitosis in transfected cells, flow cytometric analysis was carried out of *Hmgn2*-transfected cells using anti-phosphorylated histone H3 at Ser^{10} (phospho-H3), an indicator of late G_2 to anaphase in the cells with 4N content of DNA. There was no significant difference at day 2 of culture in the percentage of mitotic cells between *Hmgn2*-transfected cells and mock control (6.3 and 6.1% respectively $P>0.05$; Figure 3C).

3.4. Hmgn2 expression antagonizes erythroid cell differentiation in FL

Hmgn2 expression in FL was down-regulated during erythroid differentiation (Figure 1A). To investigate whether Hmgn2 functions in erythroid differentiation in FL as well as erythroleukaemia cells, *Hmgn2* was ectopically expressed in MNCs isolated from FL at 12.5 dpc. Two days after transfection by electroporation, CD71$^+$/Ter119$^-$ cells expressing Hmgn2, as indicated by GFP

positivity, were sorted and cultured in the presence of SCF, IL-3 and EPO for 7 days. Flow cytometry showed that the percentage of c-Kit$^+$/CD71$^+$ cells in *Hmgn2*-transfected cells (26%) was higher than that seen in mock controls (15.2%), while the percentage of CD71$^+$/Ter119$^+$ cells in *Hmgn2*-transfected cells (68.4%) was lower than in mock controls (73.6%; Figure 4A). *Gata1* expression levels were 4.2-fold lower in *Hmgn2*-transfected cells than in mock controls, and *Klf1* expression was undetectable in *Hmgn2*-transfected cells (Figure 4B). These results indicate that ectopic expression of *Hmgn2* inhibits erythroid differentiation in mouse FL.

4. Discussion

Hmgn2 is ubiquitously expressed and down-regulated during the differentiation of several cell types in vertebrates (Crippa et al., 1991; Shakoori et al., 1993; Lehtonen and Lehtonen, 2001).

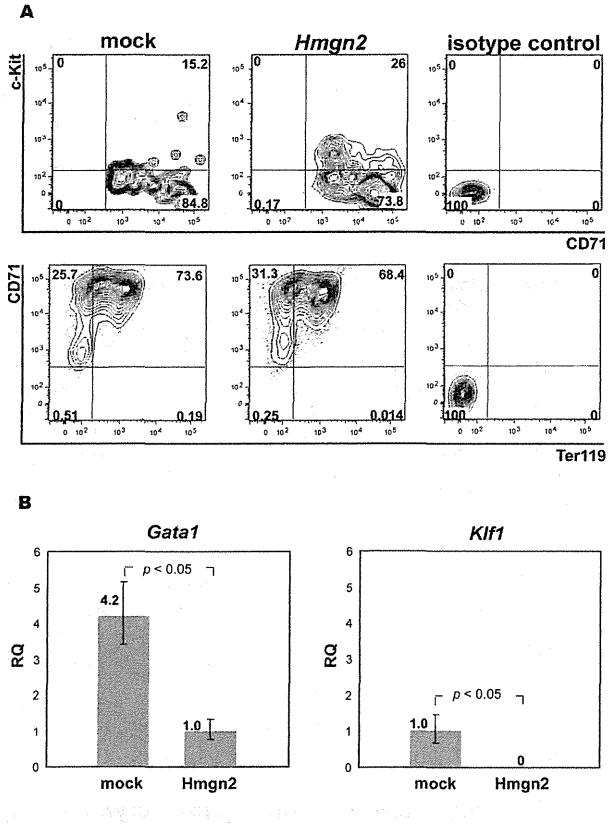

Figure 4 Ectopic expression of *Hmgn2* suppresses differentiation of erythroid progenitor cells by down-regulating *Gata1*

(**A**) Flow cytometric analysis of erythroid cells of FL MNCs transfected with *Hmgn2*/GFP expression vector. Two days after electroporation, GFP$^+$ CD71$^+$/Ter119$^-$ cells were sorted and cultured in the presence of SCF, IL-3 and EPO for 7 days. The percentage of c-Kit$^+$/CD71$^+$ cells in *Hmgn2*-transfected cells (26%) was higher than that seen in mock-transfected cells (15.2%), whereas the percentage of CD71$^+$/Ter119$^+$ cells in *Hmgn2*-transfected cells (68.4%) was lower than that seen in mock-transfected cells (73.6%). (**B**) Expression levels of *Gata1* and *Klf1* in erythroid cells were determined by RT–PCR. Two days after electroporation, *Gata1* was down-regulated in *Hmgn2*-transfected CD71$^+$/Ter119$^-$ cells compared with mock controls. *Klf1* expression was not detectable in these cells. Levels of gene expression were normalized to β-actin.

Relevant to HC (haemopoietic cell) development, injection of Hmgn2 protein into *Xenopus* embryos delayed the expression of mesoderm-specific genes (Korner et al., 2003). *Hmgn2* is also reportedly down-regulated during differentiation of erythroid cells in chicken embryos (Crippa et al., 1991) and in osteoblasts of mouse embryos (Shakoori et al., 1993). However, the role of Hmgn2 in mammalian HC development has remained unclear. The pattern of Hmgn2 gene and protein expression in mice suggests a function in erythroid differentiation (Figure 1). In mouse FL, *Hmgn2* was down-regulated during differentiation of BFU-E into reticulocytes and mature erythrocytes, when globin synthesis and enucleation occurs. Hmgn2 protein was expressed in HSCs and all stages of differentiated erythroid cells, while its expression level was down-regulated as BFU-E differentiates into mature erythrocyte. Hmgn2 therefore may regulate erythroid differentiation regardless of differentiation stage.

Friend erythroleukaemia cells are characterized as cells expressing c-Kit and CD71 (Friend 1957; Moreau-Gachelin 2008). Decrease in the number of c-Kit$^+$/CD71$^+$ cells (equivalent to CFU-E) and increase in c-Kit$^+$/CD71$^-$ cells (equivalent to BFU-E), in addition to down-regulation of *Gata1* and *Klf1* after transfection with *Hmgn2,* strongly suggest that Hmgn2 suppresses erythroid differentiation of Friend erythroleukaemia cells. During erythroid differentiation, Gata1 induces expression of CD71 and controls *Klf1* expression (Welch et al., 2004). Decrease in the number of c-Kit$^+$/CD71$^+$ cells and down-regulation of *Klf1* could be due to *Gata1* down-regulation (Figure 2A). We also showed that ectopic expression of *Hmgn2* in CD71$^+$/Ter119$^-$ FL MNCs suppresses their differentiation, indicated by the low percentage of CD71$^+$/Ter119$^+$ cells (CFU-E) and the high percentage of c-Kit$^+$/CD71$^-$ cells (BFU-E), accompanied by *Gata1* and *Klf1* down-regulation. These results are compatible with those seen in Friend erythroleukaemia cells and suggest that Hmgn2 suppresses erythroid differentiation in mice. Friend erythroleukaemia cells are comprised of c-Kit$^+$/CD71$^+$ and c-Kit$^-$/CD71$^+$ cells, equivalent to CFU-E and relatively mature cells (proerythroblasts and erythrocytes) respectively (Friend 1957; Moreau-Gachelin 2008; Supplementary Figure S4 available at http://www.cellbiolint.org/cbi/036/cbi0360195add.htm). Decrease of c-Kit$^+$/CD71$^+$ cells and increases of c-Kit$^+$/CD71$^-$, c-Kit$^-$/CD71$^+$ and c-Kit$^-$/CD71$^-$ cells were observed after transfection with *Hmgn2,* implying that differentiation arrest occurred at CFU-E. In mouse FL, expression level of *Hmgn2* declined from CFU-E to proerythroblast ($P<0.05$; Figure 1A). Hmgn2 may therefore function particularly at CFU-E during erythroid differentiation.

To investigate how Hmgn2 down-regulates erythroid differentiation, we analysed cell cycle status and related gene expression in *Hmgn2*-misexpressing cells. Following *Hmgn2* transfection at 2 and 8 days of culture, the percentage of Friend erythroleukaemia cells in S-phase increased, whereas the percentage of cells in G_1 decreased (Figure 3A). Cyclins D1 and D2 are G_1 phase-specific cyclins predominantly expressed in human, chicken and mouse erythroid cells (Dolznig et al., 1995; Dai et al., 2000). Observation of down-regulation of *cyclin D1* and *cyclin D2* genes 2 days after *Hmgn2* transfection is compatible with a low percentage of cells in G_1 and a high percentage in S-phase (Yang et al., 2006). Hmgn2 reportedly enhances DNA

replication of M13 DNA containing SV40 (simian virus 40) origin *in vitro* (Vestner et al., 1998). The data suggests that Hmgn2 does not function in mitosis of Friend erythroleukaemia cells (Figure 3C). It will be necessary to investigate whether Hmgn2 functions in mitosis during erythroid differentiation.

During erythroid differentiation, erythroblasts lose their proliferation capability and exit the cell cycle (Buttitta and Edgar, 2007) and condense chromatin. However, we do not know what is the key regulator underlying these molecular mechanisms. Our novel finding is that Hmgn2 is involved in erythroid differentiation. Therefore, further study of Hmgn2 should enable us to investigate the role of DNA replication and cell mitosis in erythroid differentiation. In conclusion, Hmgn2 appears to reduce compaction of chromatin fibres and facilitates accessibility of DNA polymerase to nucleosomes, enhancing DNA synthesis (Vestner et al., 1998; Bustin, 2001). An increase in the number of Friend erythroleukaemia cells in S-phase and a decrease of those in G_1 after *Hmgn2* misexpression might be due to enhanced DNA replication and/or blocking entry of mitosis in S-phase that promotes down-regulation of erythroid differentiation.

5. Conclusion

We have shown that ectopic expression of *Hmgn2* altered differentiation of mouse erythroid cells *in vitro*. In Friend erythroleukaemia cells, a decrease in relatively mature c-Kit$^+$/CD71$^+$ erythroid cells and an increase in immature c-Kit$^+$ CD71$^-$ erythroid cells occurred, whereas in FL HCs there was also a decrease in relatively mature CD71$^+$/Ter119$^+$ erythroid cells and an increase in relatively immature c-Kit$^+$/CD71$^+$ erythroid cells. An increase in the number of S-phase cells and a decrease in the number of G_1-phase cells in erythroleukaemia suggests that Hmgn2 antagonizes mouse erythroid differentiation may be due to enhancement of DNA replication and/or blocking entry of mitosis in S-phase.

Author Contribution

Kasem Kulkeaw performed the research and wrote the manuscript. Tomoko Inoue, Chiyo Mizuochi, Yuka Horio and Yasushi Ishihama performed the research. Daisuke Sugiyama designed and performed the research and wrote the manuscript.

Acknowledgements

We thank the Research Support Center, the Graduate School of Medical Sciences and Kyushu University for technical support; Dr K. Akashi and Dr K. Tani for helpful discussion; Dr K. Srinoun, Miss S. Okayama, Miss B. Batchuluun and Mr T. Sasaki for technical support in our laboratory; and Dr E. Lamar for critical reading of the manuscript.

Funding

Funding of this research was supported in part by the Project for Realization of Regenerative Medicine, Special Coordination Funds for Promoting Science and Technology of the Ministry of Education Culture, Sports, Science and Technology, Japan, and by a Health and Labour Sciences Research Grant from the Ministry of Health, Labour and Welfare, Japan. K.K. is a recipient of a fellowship supported by the Tokyo Biochemical Research Foundation.

References

Amen M, Espinoza HM, Cox C, Liang X, Wang J, Link TM et al. Chromatin-associated HMG-17 is a major regulator of homeodomain transcription factor activity modulated by Wnt/b-catenin signaling. Nucleic Acids Res 2008;36:462–76.

Bustin M. Regulation of DNA-dependent activities by the functional motifs of the high-mobility-group chromosomal proteins. Mol Cell Biol 1999;19:5237–46.

Bustin M. Chromatin unfolding and activation by HMGN(*) chromosomal proteins. Trends Biochem Sci 2001;26:431–7.

Bustin M, Reeves R. High-mobility-group chromosomal proteins: architectural components that facilitate chromatin function. Prog Nucleic Acids Res Mol Biol 1996;54:35–100.

Buttitta LA, Edgar BA. Mechanisms controlling cell cycle exit upon terminal differentiation. Curr Opin Cell Biol 2007;19:697–704.

Crippa MP, Nickol JM, Bustin M. Differentiation-dependent alteration in the chromatin structure of chromosomal protein HMG-17 gene during erythropoiesis. J Mol Biol 1991;217:75–84.

Dai MS, Mantel CR, Xia ZB, Broxmeyer HE, Lu L. An expansion phase precedes terminal erythroid differentiation of hematopoietic progenitor cells from cord blood *in vitro* and is associated with up-regulation of cyclin E and cyclin-dependent kinase 2. Blood 2000;96:3985–7.

Dolznig H, Bartunek P, Nasmyth K, Mullner EW, Beug, H. Terminal differentiation of normal chicken erythroid progenitors: shortening of G_1 correlates with loss of D-cyclin/cdk4 expression and altered cell size control. Cell Growth Diff 1995;6:1341–52.

Dzierzak E, Medvinsky A, De Bruijn M. Qualitative and quantitative aspects of haematopoietic cell development in the mammalian embryo. Immunol Today 1998;19:228–36.

Ema H, Nakauchi H. Expansion of hematopoietic stem cells in the developing liver of a mouse embryo. Blood 2000;95:2284–8.

Friend C. Cell-free transmission in adult Swiss mice of a disease having the character of a leukemia. J Exp Med 1957;105:307–18.

Hattangadi SM, Burke KA, Lodish HF. Homeodomain-interacting protein kinase 2 plays an important role in normal terminal erythroid differentiation. Blood 2010;115:4853–61.

Inoue T, Sugiyama D, Kurita R, Oikawa T, Kulkeaw K, Kawano H et al. APOA-1 is a novel marker of erythroid cell maturation from hematopoietic stem cells in mice and humans. Stem Cell Rev 2011;7:43–52.

Korner U, Bustin M, Scheer U, Hock R. Developmental role of HMGN proteins in Xenopus laevis. Mech Dev 2003;120:1177–92.

Lehtonen S, Lehtonen E. HMG-17 is an early marker of inductive interactions in the developing mouse kidney. Differentiation 2001;67:154–63.

McGrath K, Palis J. Ontogeny of erythropoiesis in the mammalian embryo. Curr Top Dev Biol 2008;82:1–22.

Mohamed OA, Bustin M, Clarke HJ. High-mobility group proteins 14 and 17 maintain the timing of early embryonic development in the mouse. Dev Biol 2001;229:237–49.

Moreau-Gachelin F. Multi-stage Friend murine erythroleukemia: molecular insights into oncogenic cooperation. Retrovirology 2008;5:99.

Shakoori AR, Owen TA, Shalhoub V, Stein JL, Bustin M, Stein GS et al. Differential expression of the chromosomal high mobility group proteins 14 and 17 during the onset of differentiation in mammalian osteoblasts and promyelocytic leukemia cells. J Cell Biochem 1993;51:479–87.

Shirakawa H, Herrera JE, Bustin M, Postnikov Y. Targeting of high mobility group-14/-17 proteins in chromatin is independent of DNA sequence. J Biol Chem 2000;275:37937–44.

Sugiyama D, Tsuji K. Definitive hematopoiesis from endothelial cells in the mouse embryo; a simple guide. Trends Cardiovasc Med 2006;16:45–9.
Taylor WR. FACS-based detection of phosphorylated histone H3 for the quantitation of mitotic cells. Methods Mol Biol 2004;281:293–9.
Trieschmann L, Alfonso PJ, Crippa MP, Wolffe AP, Bustin M. Incorporation of chromosomal proteins HMG-14/-17 into nascent nucleosomes induces an extended chromatin conformation and enhances the utilization of active transcription complexes. EMBO J 1995a;14:1478–89.
Trieschmann L, Postnikov Y, Rickers A, Bustin M. Modular structure of chromosomal proteins HMG-14/-17: definition of a transcriptional activation domain distinct from the nucleosomal binding domain. Mol Cell Biol 1995b;15:6663–9.
Ueda T, Catez F, Gerlitz G, Bustin M. Delineation of the protein module that anchors HMGN proteins to nucleosomes in the chromatin of living cells. Mol Cell Biol 2008;28:2872–83.
Vestner B, Bustin M, Gruss C. Stimulation of replication efficiency of a chromatin template by chromosomal protein HMG-17. J Biol Chem 1998;273:9409–14.
Weissman IL. Stem cells: units of development, units of regeneration, and units in evolution. Cell 2000;100:157–68.
Welch JJ, Watts JA, Vakoc CR, Yao Y, Wang H, Hardison RC et al. Global regulation of erythroid gene expression by transcription factor GATA-1. Blood 2004;104:3136–47.
Yang K, Hitomi M, Stacey DW. Variations in cyclin D1 levels through the cell cycle determine the proliferative fate of a cell. Cell Div 2006;1:32.

Received 18 March 2011/25 July 2011; accepted 12 October 2011

Published as Immediate Publication 12 October 2011, doi 10.1042/CBI20110169

Stem Cell Rev and Rep (2011) 7:958–968
DOI 10.1007/s12015-011-9249-3

Variation in Mesodermal and Hematopoietic Potential of Adult Skin-derived Induced Pluripotent Stem Cell Lines in Mice

Tomoko Inoue · Kasem Kulkeaw · Satoko Okayama · Kenzaburo Tani · Daisuke Sugiyama

Published online: 19 March 2011

Abstract Induced pluripotent stem cells (iPSCs) are a promising tool for regenerative medicine. Use of iPSC lines for future hematotherapy will require examination of their hematopoietic potential. Adult skin fibroblast somatic cells constitute a source of iPSCs that can be accessed clinically without ethical issues. Here, we used different methods to compare mesodermal and hematopoietic potential by embryoid body formation of five iPSC lines established from adult mouse tail-tip fibroblasts (TTFs). We observed variation in proliferation and in expression of genes (*Brachyury, Tbx1, Gata1, Klf1, Csf1r*) and proteins (Flk1, Ter119 and CD45) among TTF-derived lines. 256H18 iPSCs showed highest proliferation and most efficient differentiation into mesodermal and hematopoietic cells, while expression levels of the pluripotency genes *Oct3/4, Sox2, Klf4* and *Nanog* were lowest among lines analyzed. By contrast, the 212B2 line, transduced with *c-Myc*, showed lowest proliferation and differentiation potential, although expression levels of *Oct3/4, Sox2* and *Klf4* were highest. Overall, we find that mesodermal and hematopoietic potential varies among iPSCs from an identical tissue source and that *c-Myc* expression likely underlies these differences.

Electronic supplementary material The online version of this article (doi:10.1007/s12015-011-9249-3) contains supplementary material, which is available to authorized users.

T. Inoue · K. Kulkeaw · S. Okayama · D. Sugiyama (✉)
Department of Hematopoietic Stem Cells, SSP Stem Cell Unit,
Kyushu University Faculty of Medical Sciences,
Station for Collaborative Research 1 4F,
3-1-1 Maidashi, Higashi-Ku, Fukuoka 812–8582, Japan
e-mail: ds-mons@yb3.so-net.ne.jp

T. Inoue · K. Tani
Department of Molecular Genetics,
Medical Institute of Bioregulation, Kyushu University,
Fukuoka 812–8582, Japan

Keywords Induced pluripotent stem cells · Tail-tip fibroblasts · Embryoid body · Mesodermal induction · Hematopoietic potential

Introduction

Hematopoietic stem cells (HSCs) are already in use for transplantation therapy for hematological diseases. However, problems associated with HSC transplantation remain, such as a shortage of donors or immunoreactivity caused by HLA mismatching (rejection and graft versus host disease (GVHD)). To overcome these issues, induced pluripotent stem cells (iPSCs) could serve to generate autologous HSCs without the need for a donor. iPSCs have been established from various somatic cells by forced expression of defined factors [1, 2]. These cells display properties similar to embryonic stem cells (ESCs) in terms of differentiation capacity into various cell types, teratoma formation in immuno-deficient mice, and generation of chimeric mice with germ line transmission [3]. Therefore, iPSC technology could enable us to generate cells for clinical purposes without an embryonic source or a donor [4, 5]. Generally, *Oct3/4*, *Sox2*, *Klf4*, and *c-Myc* are retrovirally transduced into somatic cells to initiate reprogramming and establish iPSC lines. Since both expression of the *c-Myc* oncogene and retroviral infection are associated with malignancy, investigators have devised reprogramming protocols lacking *c-Myc* transduction [6] or avoiding use of non-integrated viral vectors [7] or plasmids [8] for gene delivery. Various novel approaches, including combining transcription factors and reporters, have been employed to reprogram various types of somatic cells, such as mouse embryonic fibroblasts (MEFs), adult fibroblasts, pancreatic β-cells, hepatocytes, gastric epithelial cells, B cells, and $CD34^+$ cord blood cells

[9–11]. Among these cell types, adult skin fibroblasts are a desirable potential source of somatic cells, since they can be clinically accessed without ethical problems. To help devise future clinical transplantation therapies, it is necessary to determine which iPSCs derived from tail-tip fibroblasts (TTFs) (adult skin fibroblasts in mice) are most fit to generate HSCs.

Previously, we reported variation in hematopoietic potential among several iPSC lines, regardless of the source of somatic cells [12]. This observation suggested that variation in hematopoietic potential could occur among TTF-derived iPSCs. To address this issue, we analyzed mesodermal and hematopoietic potential in five TTF-derived iPSC lines established using different transcription factors (*Oct3/4, Sox2* and *Klf4* with or without *c-Myc*) or reporter genes (*DsRed* or *GFP*). We demonstrate that both mesodermal and hematopoietic cell number and expression of mesoderm and hematopoietic cell differentiation markers varies among the five lines. Interestingly, 212B2 iPSCs, the only line created via *c-Myc* transduction, exhibited lower capacity to differentiate into mesodermal and hematopoietic cells compared than did the other four iPSCs.

Materials and Methods

iPSCs Maintenance

We used the five lines of tail-tip fibroblast (TTF)-derived iPSCs, such as 256H13, 256H18, 212B2, 212D1 and 335D1, which were kindly provided by Dr. Shinya Yamanaka (Kyoto University). These iPSCs were established by "separate method" as previously described [6]. Briefly, pMX-Oct3/4, pMX-Klf4, pMX-Sox2, and/or pMX-c-Myc plasmids were separately transfected into separate dishes of Plat-E cells using Fugene 6 reagent (Roche Applied Science, Indianapolis, IN). Twenty-four hours after transfection, the medium was replaced with serum-containing DMEM. After 24 h, each virus-containing supernatant was mixed and used for retroviral infection. Concerning iPSCs generation, TTFs were isolated from adult Nanog-GFP-IRES-Puro^r reporter mice or adult DsRed-transgenic mice. For the four-factor transduction, retrovirus-containing supernatants for *Klf4*, *c-Myc*, *Oct3/4*, *Sox2* and *DsRed*, were mixed with the ratio of 1:1:1:1:4. When the fibroblasts were transduced with the three factors, retrovirus-containing supernatants for *Klf4*, *Oct3/4*, *Sox2*, *DsRed* and Mock were mixed with the ratio of 1:1:1:1:4. For transfection, TTFs were seeded at 8.0×10^5 cells in 100-mm dish, without feeder cells. TTFs were incubated in the virus/polybrene-containing supernatants for 24 h. Four days after transduction, TTFs transduced with the three factors were reseeded at 3.5×10^5 cells per 100-mm dish with SNL feeder cells and cultured with ES medium containing DMEM, 15% FBS, 0.1 mM non essential amino acid, 0.1 mM 2-mercaptoethanol (2-ME) and 1000U/ml mouse leukemia inhibitory factor (LIF). TTFs transduced with the four factors were reseeded at 0.5×10^5 cells per 100-mm dish with feeder cells. Thirty to forty days after transduction, the colonies were selected for expansion. Drug selection with puromycin (1.5 μg/ml) was done for 212B2, 212D1 and 335D1 iPSCs. 256H13 and 256H18 iPSC lines were established without drug selection [6]. Twenty to thirty percent efficiency was achieved in transfection of all five iPSC lines.

We firstly expanded these iPSC lines with mitomycin-C (MMC)-treated mouse embryonic fibroblasts (MEFs) in StemMedium (DS Pharma Biomedical, Hyogo, Japan) containing 0.1 mM 2-ME (Nacalai Tesque, Inc., Kyoto, Japan) and 1000 U/ml mouse LIF (prepared in Dr. Minetaro Ogawa's Laboratory). The passage number (P) for each line used in this study was as follows; 256H13 (P.6-P.9), 256H18 (P.8-P.10), 212B2 (P.9), 212D1 (P.6), and 335D1 (P.8-P.10).

Fig. 1 Comparison of five iPSC lines during EB culture. **a** TTF-derived iPSCs. Morphology of five iPSC lines maintained on mitomycin-C (MMC)-treated mouse embryonic fibroblasts (MEFs) is shown by phase contrast and DsRed or GFP fluorescence. 256H13 and 256H18 iPSCs constitutively express DsRed under control of the *β-actin* (*Actb*) promoter, while 212B2, 212D1 and 335D1 iPSCs express GFP under control of the *Nanog* promoter. Scale bars are 200 μm. **b** Cell morphology during iPSC differentiation. Differentiation of iPSCs at days 4, 5, and 6. Phase contrast images. Scale bars are 100 μm. **c** Total number of viable cells from each of five lines during the course of EB formation. Four, five and six days after EB formation, differentiated-iPSCs were collected and viable cells counted using Trypan blue dye

Embryoid Body (EB) Formation

Before EB formation, iPSCs were separated from feeder cells by 0.5-hour incubation to eliminate the attached MEF cells. Then, iPSCs expressing stage-specific embryonic antigen-1 (SSEA-1) were purified by magnetic cell separation (MACS, Miltenyi Biotec, Auburn, CA). iPSCs (6×10^4 cells) were cultured in 3 ml of EB medium, which contains Iscove's Modified Dulbecco's Medium (IMDM, SIGMA-ALDRICH, St. Louis, MO) containing 15% FBS (a pre-selected batch showing the highest efficiency in inducing hematopoietic cells), 2 mM L-glutamine (SIGMA-ALDRICH), 0.0026% (vol/vol) monothioglycerol (MTG; Wako Pure Chemical Industries, Osaka, Japan), 50 μg/ml L-ascorbic acid (Wako Pure Chemical Industries), 10 U/ml penicillin, and 10 μg/ml streptomycin (SIGMA-ALDRICH).

For mesodermal cell differentiation, no cytokine was added in the EB medium. Petri dishes (60-mm in diameter, Kord-Valmark™, Ontario, Canada) were used to generate EBs. On culture days 4, 5, and 6, cells were collected by gentle pipetting, washed once in PBS, and then incubated in

a

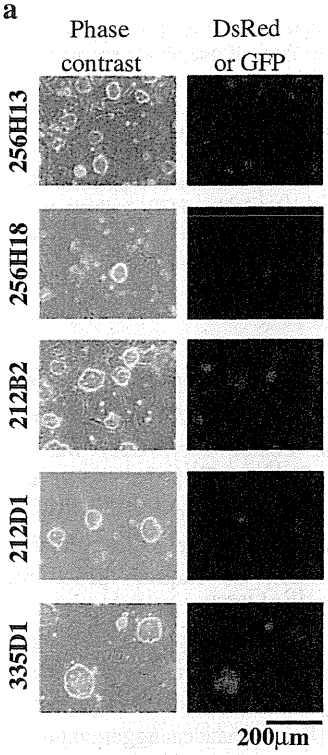

iPSC line	Transduced genes	Reporter gene	Transduction method	Viral vector	Genetic selection
iPS-TTF-FB/DsRed-256H13	Oct3/4, Klf4, Sox2	Actb-DsRed	Retrovirus	pMX-Oct3/4 pMX-Klf4 pMx-Sox2	w/o
iPS-TTF-FB/DsRed-256H18	Oct3/4, Klf4, Sox2	Actb-DsRed	Retrovirus	pMX-Oct3/4 pMX-Klf4 pMX-Sox2	w/o
iPS-TTF-FB/Ng-212B2	Oct3/4, Klf4, Sox2, c-Myc	Nanog-GFP	Retrovirus	pMX-Oct3/4 pMX-Klf4 pMX-Sox2 pMX-c-Myc	Nanog
iPS-TTF-FB/Ng-212D1	Oct3/4, Klf4, Sox2	Nanog-GFP	Retrovirus	pMX-Oct3/4 pMX-Klf4 pMX-Sox2	Nanog
iPS-TTF-FB/Ng-335D1	Oct3/4, Klf4, Sox2	Nanog-GFP	Retrovirus	pMX-Oct3/4 pMX-Klf4 pMX-Sox2	Nanog

b

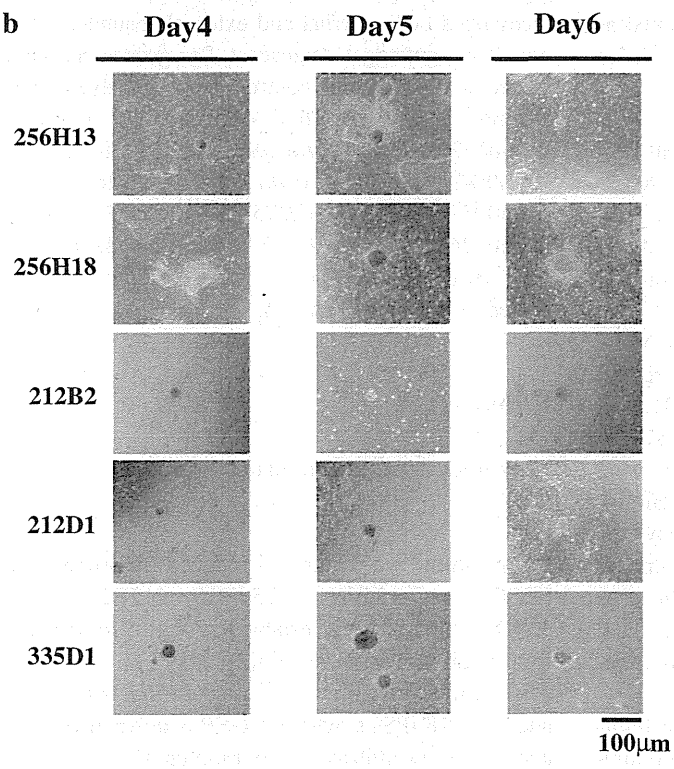

c

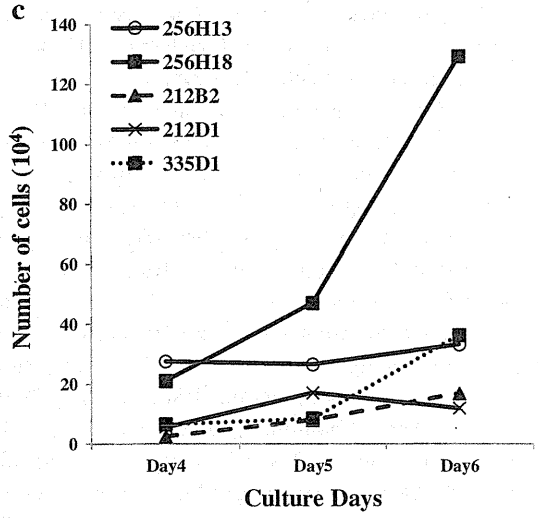

Cell Dissociation Buffer (Life Technologies, Carlsbad, CA) at 37°C for 30 min. An equal volume of medium containing 10% FBS was added and mixed gently by pipetting, and the cell suspension was passed through a 40-μm nylon mesh. The number of living cells was determined by staining with 0.4% Trypan blue (Life Technologies). For hematopoietic cell differentiation, SCF (stem cell factor), IL (interleukin)-3, EPO (erythropoietin), IL-6 and G-CSF (granulocyte colony-stimulating factor) were added in the EB medium. Petri dishes were used to generate EBs. On culture days 9, cells were collected and counted as mentioned above.

Flow Cytometry

To analyze mesodermal cells from iPSCs, cells cultured for 4, 5, and 6 days were collected as mentioned in 'EB formation' and stained with an APC-conjugated anti-CD324 (E-cadherin) antibody (Ab) (Alexa Fluor®647, eBioscience, San Diego, CA), a Pacific Blue™ -conjugated anti-mouse Flk1 (VEGFR2) Ab (BioLegend, San Diego, CA), a biotin-conjugated anti-mouse CD140α (PDGFRα) Ab (eBioscience) and an APC-Cy7-conjugated streptavidin (BD Biosciences, San Jose, CA). Biotin-conjugated antibody was used as a primary antibody and fluorescence-conjugated streptavidin was used as a secondary reagent, respectively. E-cadherin$^-$/Flk1$^+$ cells were defined as lateral mesodermal cells and E-cadherin$^-$/PDGFRα$^+$ cells as paraxial mesodermal cells, respectively.

To analyze hematopoietic cells from iPSCs, cells cultured for 9 days were collected as mentioned in 'EB formation' section and stained with an APC-Cy7-conjugated anti-mouse Ter119 Ab (eBioscience), a PB-conjugated anti-mouse CD45 Ab (BioLegend), an APC-conjugated anti-mouse F4/80 (BioLegend), a biotin-conjugated anti-mouse Gr-1 Ab (eBioscience) and PE-Cy7-conjugated streptavidin (BD Biosciences). For Mac1 Ab, a PE-conjugated anti-mouse Mac1 Ab (BioLegend) was used for GFP-expressing iPSCs (212B2, 212D1, and 335D1). And a biotin-conjugated anti-mouse Mac1 Ab (eBioscience) and a PE-Cy7-conjugated streptavidin were used for DsRed-expressing iPSCs, respectively. Biotin-conjugated antibody was used as a primary antibody and fluorescence-conjugated streptavidin was used as a secondary reagent, respectively. Ter119 positive cells were defined as erythroid cells, CD45 positive cell as leukocytes, Mac1$^+$/F4/80$^+$ cells as macrophages and Gr-1$^+$/F4/80$^-$ cells as granulocytes, respectively.

To stain dead cells, propidium iodide (PI, Life Technologies, Eugene, Oregon) was used for GFP-expressing iPSCs, and TO-PRO®-1 iodide (Life Technologies) was used for DsRed-expressing iPSCs. Cells were analyzed using a FACS Aria cell sorter (Becton Dickinson, Franklin Lakes, NJ). Data files were analyzed using FlowJo software (Tree Star, San Carlos, CA).

Fig. 2 Mesodermal cell differentiation from iPSCs. **a** Flow cytometric analysis of mesodermal cells from all five iPSC lines at days 4, 5, and 6 during the course of EB culture. Lateral mesodermal cells were evaluated based on lack of expression of the surface marker E-cadherin (CD324, epithelial cadherin) and expression of Flk1 (CD309, VEGFR2) (*upper panel*). Paraxial mesodermal cells were evaluated based on lack of expression of E-cadherin and expression of PDGFRα (*lower panel*). **b** Quantitative real-time PCR analysis was used to detect the mesodermal markers *Flk1*, *Tbx6* and *Brachyury* at day 4 of EB culture. Data was normalized to *β-actin* expression

Quantitative Real-Time PCR

Total RNA was isolated with the RNAqueous-Micro Kit (Ambion, Austin, TX). A high-capacity cDNA Archive kit (Applied Biosystems, Foster City, CA) was used to synthesize cDNA from mRNA. mRNA levels were normalized to *β-actin* as an internal control. In real-time PCR, mRNA levels were analyzed by the SYBR Green method with gene-specific primers or Taqman probe methods. Genes analyzed by SYBR Green included *Oct3/4* (Fw; gcagctcagccttaagaacatgt, Rv; cgatttgcatatctcctgaaggt), *Klf4* (Fw; gaactcacacaggcgagaaacc, Rv; tcggagcgggcgaatt), *Sox2* (Fw; atcaggctgccgagaatcc, Rv; ctcaaactgtgcataatggagt taaaaa) and *Nanog* (Fw; caaaaccaaaggatgaagtgcaa, Rv; gtgctgagcccttctgaatca). *Oct3/4*, *Klf4*, and *Sox2* primer sets recognized both internal and external sequences. Mouse *β-actin* (Fw; gctctggctcctagcaccat, Rv; gccaccgatccacacagagt) served as an internal control. Genes analyzed using the Taqman probe (Applied Biosystems) included *Flk1* (Mm01222421_m1), *Brachyury* (Mm01318252_m1), *Tbx6* (Mm00441681_m1), *Gata1* (Mm01352636_m1), *Klf1* (Mm00516096_m1), *CD45* (Mm01293577_m1), *Csf1r* (Mm01266652_m1), *PU.1* (Mm00488142_m1), and *c-Myc* (Mm00487804_m1). Mouse *β-actin* (4352933E) served as an internal control.

Results

Morphology and EB Formation Capacity of TTF-derived iPSCs

In this study, we cultured 5 induced pluripotent stem cell (iPSC) lines—256H13, 256H18, 212B2, 212D1, and 335D1—which were established by different protocols from adult mouse tail-tip fibroblasts (TTF) [6]. The *DsRed* gene is downstream of the *β-actin* (*ACTB*) gene in 256H13 and 256H18 iPSCs, whereas *GFP* is downstream of *Nanog* and serves an indicator of pluripotency in 212B2, 212D1, and 335D1 iPSCs, as summarized in Fig. 1a. *Oct3/4*, *Klf4*, *and Sox2* genes were transduced into TTFs to establish all iPSC lines, while the 212B2 line was also transduced with *c-Myc*. All iPSC colonies exhibited round morphology and exhibited large nucleoli and low cytoplasmic content.

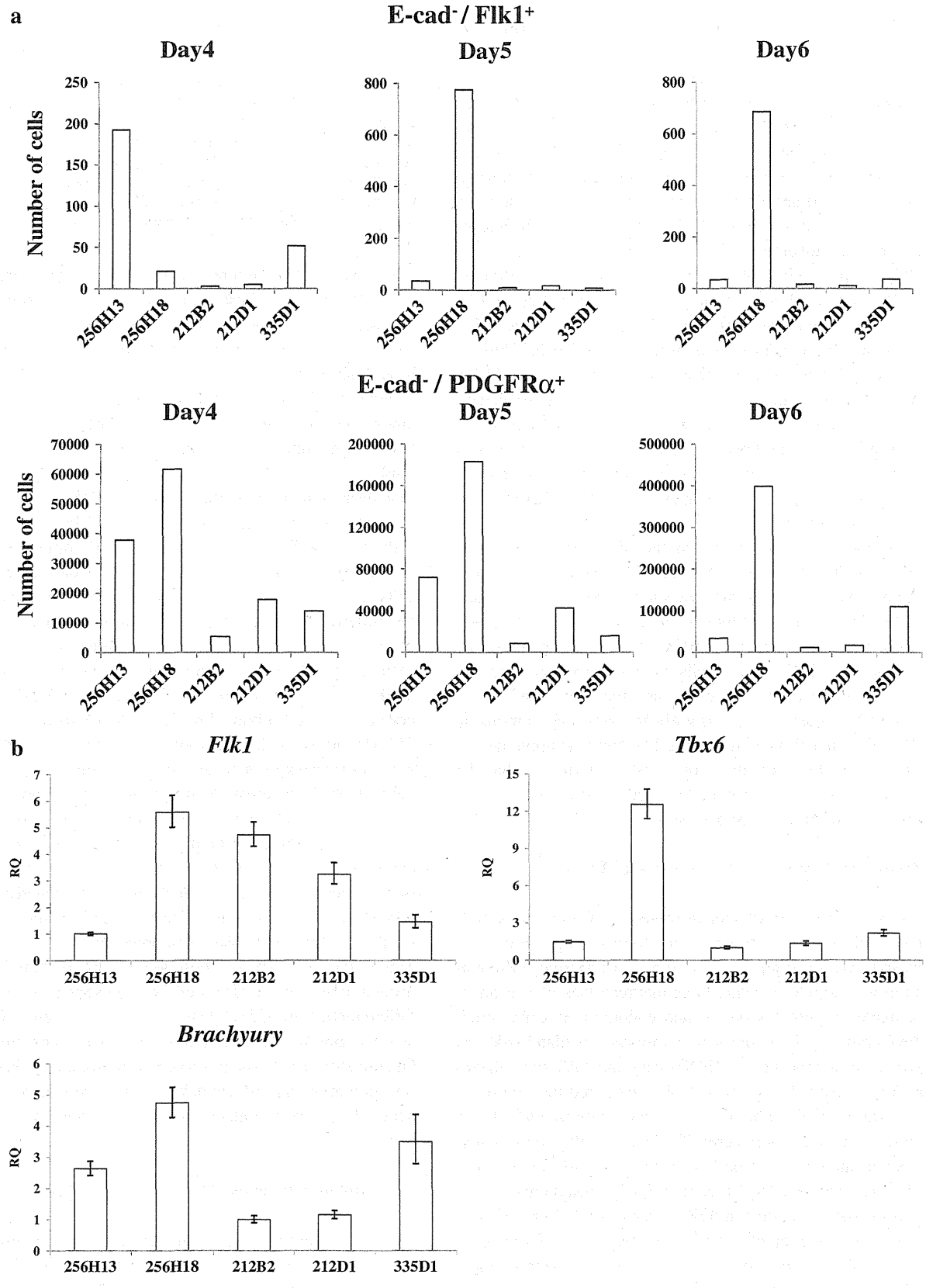
a
E-cad⁻ / Flk1⁺
Day4
Day5
Day6
Number of cells
250
200
150
100
50
0
800
600
400
200
0
256H13
256H18
212B2
212D1
335D1
E-cad⁻ / PDGFRα⁺
Day4
Day5
Day6
Number of cells
70000
60000
50000
40000
30000
20000
10000
0
200000
160000
120000
80000
40000
0
500000
400000
300000
200000
100000
0
256H13
256H18
212B2
212D1
335D1
b
Flk1
Tbx6
Brachyury
RQ
7
6
5
4
3
2
1
0
15
12
9
6
3
0
256H13
256H18
212B2
212D1
335D1

335D1 formed larger colonies than other lines (Fig. 1a). 212B2, 212D1and 335D1 lines were GFP-positive, indicative of *Nanog* expression and pluripotency.

Next, we performed differentiation culture using the method of embryoid body (EB) formation without cytokines (Supplementary Fig. 1a). Four, five and six days after EB formation, we observed the cultured cells microscopically (Fig. 1b) and evaluated proliferation by cell counting (Fig. 1c). All iPSCs formed EBs, although EB size and the number of adherent cells varied among lines (Fig. 1b). 212B2 and 335D1 iPSCs formed round EBs, although 335D1-derived EBs were larger than 212B2-derived EBs. By contrast, cultured 256H13, 256H18 and 212D1 iPSCs gave rise to adherent cells as well as round EBs. 256H18-derived EBs were larger than those derived from 212D1 cells at day 5 and, in the case of 256H18, adherent cells were observed most frequently (Fig. 1b). In terms of proliferation, the number of 256H13-derived cells increased at day 4 (2.75×10^5 cells) and then plateaued. The number of 256H18 iPSCs also increased gradually through the culture period and then plateaued. 256H18 iPSCs-derived cells gradually increased during the culture and plateaued at day 5 (4.70×10^5 cells). Although 212B2 and 335D1 lines increased gradually during the culture period, their viable cell number at day 6 (1.69×10^5 and 3.63×10^5, respectively) was lower than that of 256H18 iPSCs. By contrast, the number of 212D2-derived cells increased from day 4 (5.50×10^4 cells) to 5 (1.70×10^5 cells), and then decreased (1.19×10^5 cells). There was no significant difference among all iPSC lines in cell viability during EB culture (Supplementary Fig. 2). Taken together, our results indicate that EB formation and cell proliferation varies among five iPSC lines derived from the same tissue.

Mesodermal Potential of TTF-derived iPSCs

To assess iPSC hematopoietic potential, we first examined their mesodermal potential, as hematopoietic cells are mesodermal in origin [13, 14]. ESC mesodermal differentiation was monitored using three markers: lack of E-cadherin (a marker of both ectoderm and endoderm in early mouse development [15]) expression, expression of platelet-derived growth factor receptor α (PDGFRα) and Flk1 (also known as VEGF receptor 2) [16, 17]. We compared the number of iPSC-derived E-cadherin$^-$/Flk1$^+$ cells, representing lateral mesoderm, and E-cadherin$^-$/PDGFRα^+ cells, representing paraxial mesoderm, at days 4, 5 and 6 of EB culture, since ESC-derived EBs [18, 19] contain Flk1$^+$ mesodermal cells at 4 to 4.5 days of culture and iPSC-derived EBs contain Flk1$^+$ cells at 5 days of culture [12]. The emergence of E-cadherin$^-$/Flk1$^+$ cells from the 256H13 line was the most rapid among the five lines tested, and the number of cells in this fraction was highest at day 4 (193 cells) and then decreased (Fig. 2a, upper panel). The number of E-cadherin$^-$/Flk1$^+$ cells from 256H18 was the highest among the five lines tested (day 5; 776 cells) (Fig. 2a, upper panel). In contrast, the number of 212B2 and 212D1 iPSC-derived E-cadherin$^-$/Flk1$^+$ cells was lower than that seen in the other three lines. The number of E-cadherin$^-$/PDGFRα^+ cells from 256H18 was highest among the five lines (day 6; 3.97×10^5 cells) (Fig. 2a, lower panel). The number of E-cadherin$^-$/PDGFRα^+ cells from 256H13 and 212D1 lines increased from days 4 to 5 and then decreased, whereas those from 256H18 and 212B2 lines gradually increased from days 4 to 6. The number of E-cadherin$^-$/PDGFRα^+ cells from 335D1 dramatically increased from day 5 (1.59×10^4 cells) to day 6 (1.10×10^5 cells) (Fig. 2a, lower panel). To confirm iPSC mesodermal cell differentiation, we employed PCR to examine expression of the mesoderm markers *Flk1* (lateral mesoderm), *Tbx6* [20] (paraxial mesoderm) and *Brachyury* [21] (pan-mesodermal marker). *Flk1* expression was lowest in 256H13-derived cells at day 4 of culture (Fig. 2b), whereas it was highest in 256H18-derived cells over days 4 to 6 (Supplementary Fig. 3 and 5). *Tbx6* expression at day 4 was highest in 256H18-derived iPSCs, whereas *Tbx6* expression was highest at days 5 and 6 in 335D1- and 256H13-derived cells, respectively (Fig. 2b and Supplementary Fig. 3 and 5). *Brachyury* expression at day 4 was higher in 256H18- and 335D1-derived cells compared to others (Fig. 2b), whereas it was highest at days 5 and 6 in 335D1- and 256H13-derived cells, similar to *Tbx6* expression (Supplementary Fig. 3 and 5). There was a trend in mesodermal differentiation. Early differentiation in 256H13 cells was observed, whereas late differentiation in 335D1 (Fig. 2a). 256H18 cells differentiated into both lateral and paraxial mesoderm most frequently. Overall differences we observed in mesodermal differentiation potential suggest variation in mesodermal potential of adult skin-derived induced pluripotent stem cell lines in mice.

Fig. 3 Hematopoietic cell differentiation from iPSCs. **a** Differentiated iPSCs were collected at day 9 of EB culture and Ter119$^+$ erythroid cells were evaluated by flow cytometry. **b** Quantitative real-time PCR analysis was used to detect expression of the erythroid genes *Gata1* and *Klf1* at day 9 of EB culture. Data was normalized to *β-actin* expression. **c**, **d** Differentiated iPSCs were collected at day 9 of EB culture and evaluated by flow cytometry for (**c**) CD45$^+$ leukocytes and (**d**) myeloid cells (Mac1$^+$/F4/80$^+$ macrophages and Gr-1$^+$/F4/80$^-$ granulocytes). **e** Quantitative real-time PCR analysis was used to detect expression of the myeloid-related genes *CD45*, *Csf1r* and *PU.1* at day 9 of EB culture. Data was normalized to *β-actin* expression

Hematopoietic Potential of TTF-derived iPSCs

Next we examined cell number and the percentage of erythroid and myeloid cells emerging during EB formation at day 9 of culture in the presence of cytokines (Supplementary Fig. 1b). Flow cytometry analysis showed that

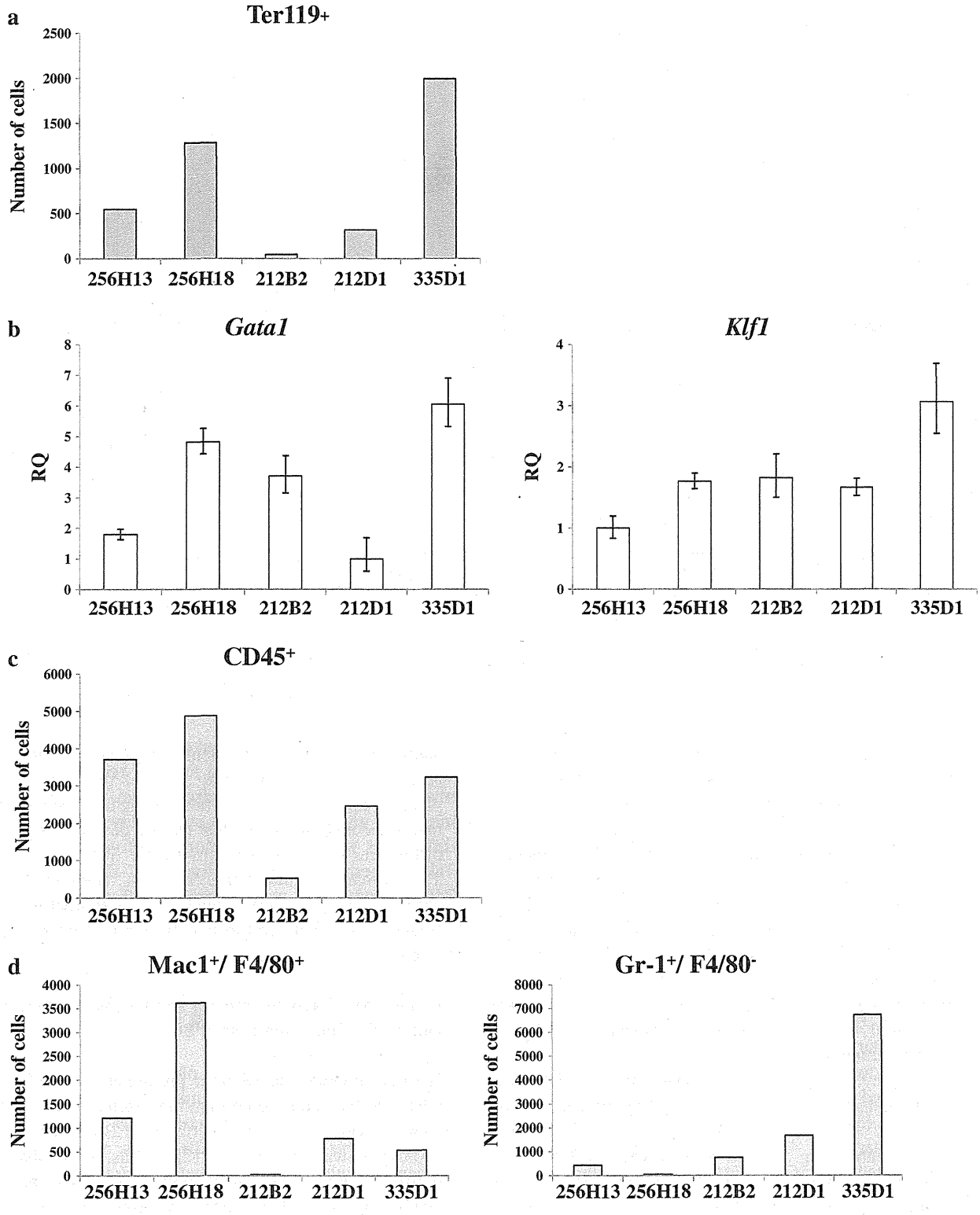
a
Ter119+
Number of cells
2500
2000
1500
1000
500
0
256H13 256H18 212B2 212D1 335D1
b
Gata1
RQ
8
7
6
5
4
3
2
1
0
256H13 256H18 212B2 212D1 335D1
Klf1
RQ
4
3
2
1
0
256H13 256H18 212B2 212D1 335D1
c
CD45+
Number of cells
6000
5000
4000
3000
2000
1000
0
256H13 256H18 212B2 212D1 335D1
d
Mac1+/ F4/80+
Number of cells
4000
3500
3000
2500
2000
1500
1000
500
0
256H13 256H18 212B2 212D1 335D1
Gr-1+/ F4/80-
Number of cells
8000
7000
6000
5000
4000
3000
2000
1000
0
256H13 256H18 212B2 212D1 335D1

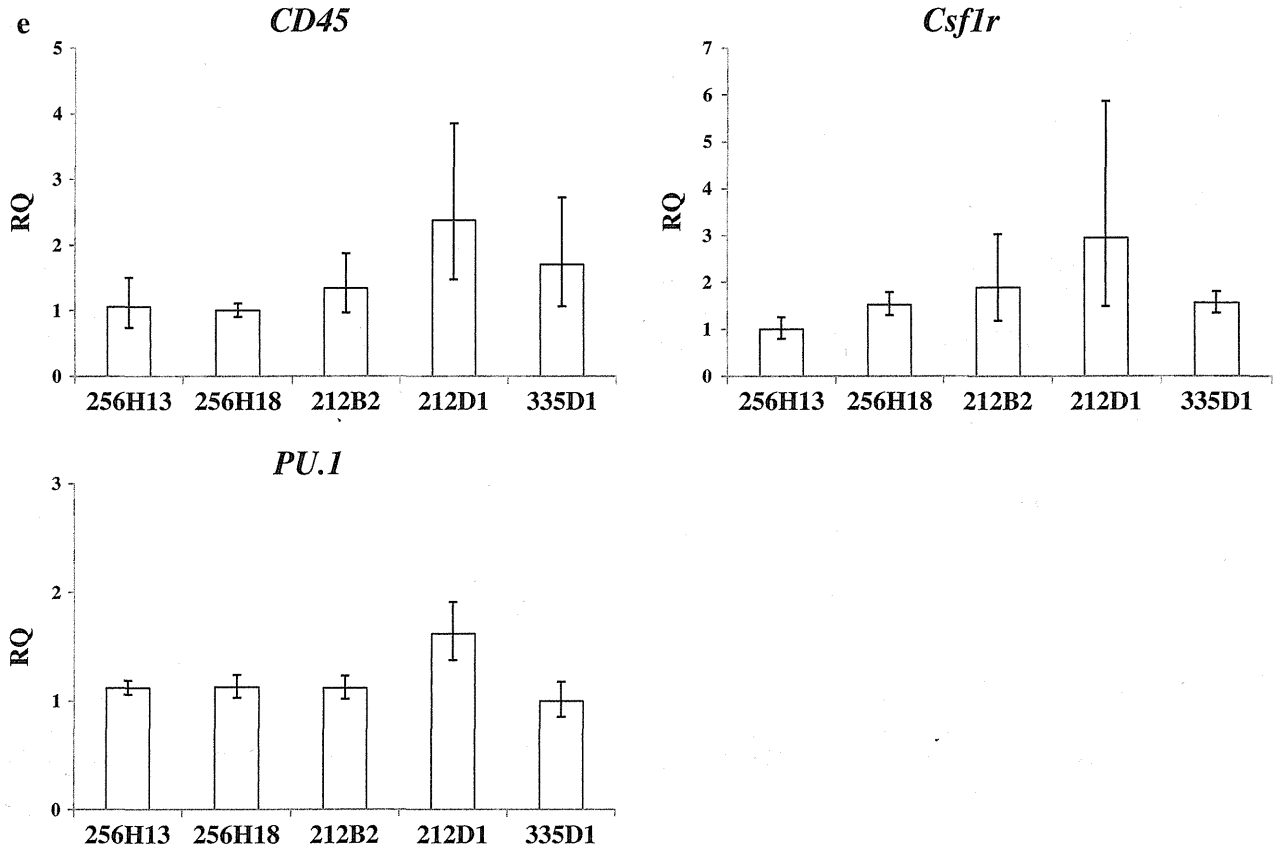

Fig. 3 (continued)

lines 256H18 and 335D1 efficiently differentiated into Ter119$^+$ erythroid cells at 0.35% (1280 cells) and 0.72% (1991 cells), respectively. By contrast, 212B2 cells differentiated into Ter119$^+$ cells at low frequency (46 cells, 0.12%) (Fig. 3a, Supplementary Fig. 4a). In agreement, real-time PCR analysis showed that expression of the erythropoietic transcription factors *Gata1* [22] and *Klf1* [23] was the highest in 335D1 cells (6.05 times higher than in 212D1 cells and 3.07 times higher than in 256H13 cells) (Fig. 3b). 256H18 and 335D1 cells differentiated into CD45$^+$ leukocytes at 1.32% (4880 cells) and 1.17% (3229 cells), respectively (Fig. 3c, Supplementary Fig. 4b).

Flow cytometry analysis showed that 256H18 cells differentiated into Mac1$^+$/F4/80$^+$ macrophages at high frequency (3622 cells, 0.98%) (Fig. 3d, left panel; Supplementary Fig. 4c, left panel), whereas 335D1 cells differentiated into Gr-1$^+$/F4/80$^-$ granulocytes at high frequency (6738 cells, 2.45%) (Fig. 3d, right panel; Supplementary Fig. 4c, right panel). By contrast, 212B2 cells, which are transduced with the *c-Myc* gene, differentiated into CD45$^+$ leukocytes, Mac1$^+$/F4/80$^+$ macrophages and Gr-1$^+$/F4/80$^-$ granulocytes at low frequency (523, 20 and 756 cells, respectively) (Fig. 3c, d). When we analyzed expression of the leukocyte marker *CD45*, *Csf1r* (encoding colony stimulating factor 1 receptor, a macrophage marker), and *PU.1* (also known as *Spi-1*, which marks the myeloid lineage) at culture day 9, no significant differences were observed among the five lines (Fig. 3e). Taken together, among the five iPSC lines tested, only 256H18 and 335D1 were capable of differentiating at high frequency into both erythroid cells and leukocytes at day 9 of culture.

Expression of Reprogramming and Pluripotency Genes During EB Formation from iPSCs

We next investigated whether pluripotency of iPSCs was related to the nature reprogramming factors used transduce somatic cells. Prior to initiating EB culture, *c-Myc* expression was highest in 212B2 cells, which had been transduced with *c-Myc* along with *Oct3/4*, *Klf4* and *Sox2* genes (Fig. 4a). *Oct3/4* gene expression was highest in 256H13 cells, whereas *Klf4*, *Sox2* and *Nanog* gene expression did not significantly differ among the lines prior to culture. *Oct3/4*, *Klf4* and *Sox2* expression at day 4 of culture was the highest in 212B2 cells, suggesting that they retain pluripotency longer than do the other lines (Fig. 4b).

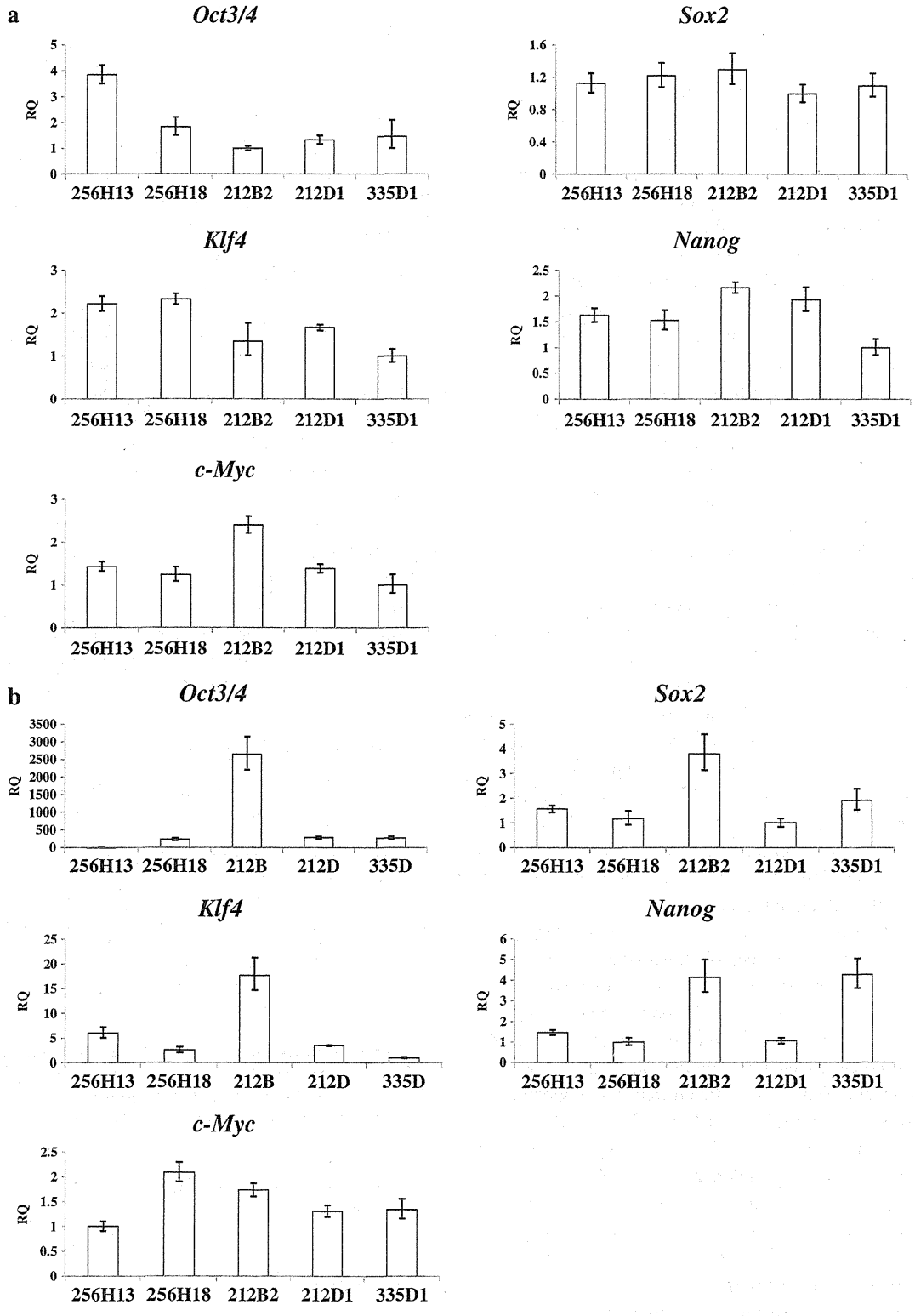

Fig. 4 Comparison of reprogramming and pluripotency gene expression. Quantitative real-time PCR analysis was used to detect expression of the reprogramming genes *Oct3/4, Klf4, Sox2* and *c-Myc* and the pluripotency gene *Nanog* at days 0 (**a**) and 4 (**b**) of EB culture. Data was normalized to *β-actin* expression

Discussion

iPSCs constitute important tools for future regenerative medicine. In this study we compared mesodermal and hematopoietic potential of several iPSC lines, since differentiation potential reportedly varies among iPSC lines established by different sources and methods [12]. Although all iPSCs possessed pluripotency, as defined by expression of *Oct3/4* and *Nanog*, each line showed variations in EB formation and cell proliferation. Examination of mesodermal potential using both flow cytometry and real-time PCR methods, confirmed these differences: specifically, the 256H18 iPSC line gave rise to mesodermal cells at high frequency, whereas 212B2 cells showed the lowest frequency. To identify factors underlying mesodermal potential, we compared expression of both differentiation and pluripotency markers. As summarized in Supplementary Fig. 5, expression of the differentiation markers *Flk1*, *Tbx6*, and *Brachyury* in 256H18 iPSCs was highest at day 4 of culture. Although there was no significant correlation between mesodermal potential and expression of pluripotency markers (Fig. 4), the number of EBs is likely positively correlated with mesodermal potential (Fig. 1). In terms of hematopoietic potential, variations in differentiation capacity were confirmed by flow cytometric and real-time PCR analyses. 256H18 and 335D1 iPSCs generated erythroid cells and leukocytes at high frequency, whereas a low frequency was seen with 212B2 cells (Fig. 3). Expression of the *Oct3/4*, *Sox2*, *Klf4* and *Nanog* pluripotency genes in 256H18 was lowest, whereas 212B2 iPSCs showed highest expression of *Oct3/4*, *Sox2* and *Klf4*. Given the results of our hematopoietic cell differentiation assays at day 4 of culture, these results suggest an inverse relationship between hematopoietic potential and pluripotency gene expression (Fig. 4). *c-Myc* expression in 212B2 cells was highest before culture (Fig. 4a), likely due to ectopic transduction of *c-Myc*. There was a correlation between high *c-Myc* expression and low induction of mesodermal and hematopoietic cells. In our culture conditions, *c-Myc* likely down-regulates mesodermal and hematopoietic cell induction from the 212B2 iPSC line. Our results are compatible with previous reports mentioning that *c-Myc* maintains pluripotency of ESCs [24] and iPSCs [25], and similar to the report showing that c-Myc down-regulates cardiogenic [26] and endodermal differentiation [25] of iPSCs. Taken together, our results imply that iPSCs lacking *c-Myc* transduction will be preferably used for clinical purposes.

Passage number of iPSCs reportedly affected the hematopoietic differentiation [27]. As passage number of iPSCs increased, the transient epigenetic memory of their original somatic cells was gradually lost and hematopoietic differentiation capacity was up-regulated in TTF-derived iPSCs [27]. 256H18 and 335D1 iPSCs generated hematopoietic cells at high frequency, whereas a low frequency was seen in 212B2 in our culture condition (Fig. 3). Since we used iPSC lines of 256H18, 335D1 and 212B2 with similar passage number (P.8- P.10), it is unlikely that passage number affected the hematopoietic differentiation capacity among these three lines. Concerning the other 2 iPSC lines, passage number was lower in 256H13 (P.6-P.9) and 212D1 (P.6) than in 256H18, 335D1 and 212B2. Less hematopoietic cell differentiation in 256H13 and 212D1 than 256H18 and 335D1 was might be due to the difference of passage number.

Taken together, even derived from the same TTF origin, each iPSC demonstrated different mesodermal and hematopoietic potential. Transduction method with retroviral infection and transfection efficiency (20–30%) were similar, while *c-Myc* gene transduction, drug selection with puromycin, reporter genes (Actb-DsRed or Nanog-GFP) and passage number were not identical among five iPSC lines. Therefore, variation in mesodermal and hematopoietic potential was likely affected by combination of transduced genes and passage number, but not transfection methods, drug selection and reporter genes.

Recently, it was reported that iPSCs can be established from peripheral blood (PB) cells [28]. Since collecting a PB sample from a patient is practically easier than taking skin fibroblasts by biopsy in terms of risk and pain, it will be further necessary to evaluate the hematopoietic potential of PB-derived iPSCs in both mice and humans.

Acknowledgements This work was supported by a grant from the Project for Realization of Regenerative Medicine from the Ministry of Education, Culture, Sports, Science and Technology and by a grant from the BASIS project from the Ministry of Education, Culture, Sports, Science and Technology. T. Inoue and K. Kulkeaw is supported by research fellowships from the Ministry of Education, Culture, Sports, Science and Technology, and from The Tokyo Biochemical Research Foundation, respectively. We thank Dr. Keisuke Okita, Ms. Yuka Horio, Ms. Chiyo Mizuochi and the Research Support Center, Graduate School of Medical Sciences, Kyushu University for technical supports, and Dr. Minetaro Ogawa and Dr. Hiroshi Sakamoto for providing LIF. All iPSCs were kindly provided by Dr. Shinya Yamanaka.

Author Contributions Tomoko Inoue performed the experiments, analyzed data and wrote the manuscript. Kasem Kulkeaw, Satoko Okayama and Kenzaburo Tani performed the experiments. Daisuke Sugiyama designed the experiments and wrote the manuscript.

Conflict of Interest All disclosures will be published when the manuscript is accepted.

References

1. Takahashi, K., & Yamanaka, S. (2006). Induction of pluripotent stem cells from mouse embryonic and adult fibroblast cultures by defined factors. *Cell, 126*, 663–676.
2. Wernig, M., Meissner, A., Foreman, R., et al. (2007). In vitro reprogramming of fibroblasts into a pluripotent ES-cell-like state. *Nature, 448*, 318–324.

3. Okita, K., Ichisaka, T., & Yamanaka, S. (2007). Generation of germline-competent induced pluripotent stem cells. *Nature, 448*, 313–317.
4. Yu, J., Vodyanik, M. A., Smuga-Otto, K., et al. (2007). Induced pluripotent stem cell lines derived from human somatic cells. *Science, 318*, 1917–1920.
5. Nelson, T. J., Martinez-Fernandez, A., Yamada, S., Mael, A. A., Terzic, A., & Ikeda, Y. (2009). Induced pluripotent reprogramming from promiscuous human stemness related factors. *Clinical and Translational Science, 2*, 118–126.
6. Nakagawa, M., Koyanagi, M., Tanabe, K., et al. (2008). Generation of induced pluripotent stem cells without Myc from mouse and human fibroblasts. *Nature Biotechnology, 26*, 101–106.
7. Stadtfeld, M., Brennand, K., & Hochedlinger, K. (2008). Reprogramming of pancreatic beta cells into induced pluripotent stem cells. *Current Biology, 18*, 890–894.
8. Okita, K., Nakagawa, M., Hyenjong, H., Ichisaka, T., & Yamanaka, S. (2008). Generation of mouse induced pluripotent stem cells without viral vectors. *Science, 322*, 949–953.
9. Aoi, T., Yae, K., Nakagawa, M., et al. (2008). Generation of pluripotent stem cells from adult mouse liver and stomach cells. *Science, 321*, 699–702.
10. Hanna, J., Markoulaki, S., Schorderet, P., et al. (2008). Direct reprogramming of terminally differentiated mature B lymphocytes to pluripotency. *Cell, 133*, 250–264.
11. Takenaka, C., Nishishita, N., Takada, N., Jakt, L. M., & Kawamata, S. (2010). Effective generation of iPS cells from CD34+ cord blood cells by inhibition of p53. *Experimental Hematology, 38*, 154–162.
12. Kulkeaw, K., Horio, Y., Mizuochi, C., Ogawa, M., & Sugiyama, D. (2010). Variation in hematopoietic potential of induced pluripotent stem cell lines. *Stem Cell Reviews, 6*, 381–389.
13. Huber, T. L., Kouskoff, V., Fehling, H. J., Palis, J., & Keller, G. (2004). Haemangioblast commitment is initiated in the primitive streak of the mouse embryo. *Nature, 432*, 625–630.
14. Lengerke, C., Grauer, M., Niebuhr, N. I., et al. (2009). Hematopoietic development from human induced pluripotent stem cells. *Annals of the New York Academy of Sciences, 1176*, 219–227.
15. Era, T., Izumi, N., Hayashi, M., Tada, S., & Nishikawa, S. (2008). Multiple mesoderm subsets give rise to endothelial cells, whereas hematopoietic cells are differentiated only from a restricted subset in embryonic stem cell differentiation culture. *Stem Cells, 26*, 401–411.
16. Kataoka, H., Takakura, N., Nishikawa, S., et al. (1997). Expressions of PDGF receptor alpha, c-Kit and Flk1 genes clustering in mouse chromosome 5 define distinct subsets of nascent mesodermal cells. *Development, Growth & Differentiation, 39*, 729–740.
17. Sakurai, H., Era, T., Jakt, L. M., Okada, M., Nakai, S., & Nishikawa, S. (2006). In vitro modeling of paraxial and lateral mesoderm differentiation reveals early reversibility. *Stem Cells, 24*, 575–586.
18. Choi, K., Kennedy, M., Kazarov, A., Papadimitriou, J. C., & Keller, G. (1998). A common precursor for hematopoietic and endothelial cells. *Development, 125*, 725–732.
19. Fehling, H. J., Lacaud, G., Kubo, A., et al. (2003). Tracking mesoderm induction and its specification to the hemangioblast during embryonic stem cell differentiation. *Development, 130*, 4217–4227.
20. Chapman, D. L., Agulnik, I., Hancock, S., Silver, L. M., & Papaioannou, V. E. (1996). Tbx6, a mouse T-Box gene implicated in paraxial mesoderm formation at gastrulation. *Developmental Biology, 180*, 534–542.
21. Wilkinson, D. G., Bhatt, S., & Herrmann, B. G. (1990). Expression pattern of the mouse T gene and its role in mesoderm formation. *Nature, 343*, 657–659.
22. Whitelaw, E., Tsai, S. F., Hogben, P., & Orkin, S. H. (1990). Regulated expression of globin chains and the erythroid transcription factor GATA-1 during erythropoiesis in the developing mouse. *Molecular and Cellular Biology, 10*, 6596–6606.
23. Miller, I. J., & Bieker, J. J. (1993). A novel, erythroid cell-specific murine transcription factor that binds to the CACCC element and is related to the Kruppel family of nuclear proteins. *Molecular and Cellular Biology, 13*, 2776–2786.
24. Varlakhanova, N. V., Cotterman, R. F., & deVries, W. N. (2010). Myc maintains embryonic stem cell pluripotency and self-renewal. *Differentiation, 80*, 9–19.
25. Smith, K. N., Singh, A. M., & Dalton, S. (2010). Myc represses primitive endoderm differentiation in pluripotent stem cells. *Cell Stem Cell, 7*, 343–54.
26. Martinez-Fernandez, A., Nelson, T. J., Ikeda, Y., & Terzic, A. (2010). c-MYC independent nuclear reprogramming favors cardiogenic potential of induced pluripotent stem cells. *Journal of Cardiovascular Translational Research, 3*, 13–23.
27. Polo, J. M., Liu, S., & Figueroa, M. E. (2010). Cell type of origin influences the molecular and functional properties of mouse induced pluripotent stem cells. *Nature Biotechnology, 28*, 848–55.
28. Loh, Y. H., Agarwal, S., & Park, I. H. (2009). Generation of induced pluripotent stem cells from human blood. *Blood, 113*, 5476–9.

Biochemical and Biophysical Research Communications 410 (2011) 301–306

Contents lists available at ScienceDirect

Biochemical and Biophysical Research Communications

journal homepage: www.elsevier.com/locate/ybbrc

Hepatoblasts comprise a niche for fetal liver erythropoiesis through cytokine production

Daisuke Sugiyama *, Kasem Kulkeaw, Chiyo Mizuochi, Yuka Horio, Satoko Okayama

Division of Hematopoietic Stem Cells, Advanced Medical Initiatives, Department of Advanced Medical Initiatives, Kyushu University Faculty of Medical Sciences, Fukuoka 812-8582, Japan

ARTICLE INFO

Article history:
Received 18 May 2011
Available online 30 May 2011

Keywords:
Hepatoblasts
Erythropoiesis
Fetal liver

ABSTRACT

In mammals, definitive erythropoiesis first occurs in fetal liver (FL), although little is known about how the process is regulated. FL consists of hepatoblasts, sinusoid endothelial cells and hematopoietic cells. To determine niche cells for fetal liver erythropoiesis, we isolated each FL component by flow cytometry. mRNA analysis suggested that Dlk-1-expressing hepatoblasts primarily expressed *EPO* and *SCF*, genes encoding erythropoietic cytokines. EPO protein was detected predominantly in hepatoblasts, as assessed by ELISA and immunohistochemistry, and was not detected in sinusoid endothelial cells and hematopoietic cells. To characterize hepatoblast function in FL, we analyzed *Map2k4*$^{-/-}$ mouse embryos, which lack hepatoblasts, and observed down-regulation of *EPO* and *SCF* expression in FL relative to wild-type mice. Our observations demonstrate that hepatoblasts comprise a niche for erythropoiesis through cytokine secretion.

1. Introduction

Hematopoiesis is the process by which pluripotent hematopoietic stem cells (HSCs) are generated, differentiate into specific progenitors, and ultimately mature into numerous blood cell types, including erythrocytes, megakaryocytes, lymphocytes, neutrophils, and macrophages [1]. In the mouse embryo, HSCs and hematopoietic progenitors (HPCs) are generated in the aortic region, known as the para-aortic Splanchnopleura (p-Sp)/Aorta–Gonad–Mesonephros (AGM) region, the yolk sac (YS), and the placenta [2–9]. In mid-gestation, hematopoiesis, particularly erythropoiesis, occurs in fetal liver (FL) [2,9,10]. Erythropoiesis has been classically described as occurring in two waves: first primitive and then definitive erythropoiesis [4]. Primitive erythropoiesis supports a transient wave of embryonic erythropoiesis in the yolk sac, while definitive erythropoiesis contributes to adult-type erythropoiesis. In mammals, definitive erythropoiesis occurs first in FL and then shifts to adult bone marrow (BM) shortly before birth [11]. There are greater numbers of erythroid progenitors, such as burst-forming unit-erythroids (BFU-E) and colony-forming unit-erythroids (CFU-E), in FL than in BM [12]. In addition, in mice, the number of mature erythroid cells in circulation dramatically increases from 12.5 to 16.5 day post-coitum (dpc), suggesting that massive expansion of both erythroid progenitors and terminally differentiated erythroid cells occurs in FL [13]. Erythropoietin (EPO) is a cytokine that regulates erythroid cell differentiation, maturation, proliferation and survival, and is primarily produced by adult kidney cells, where production is up-regulated by hypoxia [14]. Terminal proliferation and differentiation of CFU-E is stimulated by EPO, whereas BFU-E, which are more immature than CFU-E, respond to stem cell factor (SCF), insulin-like growth factor (IGF)-1, corticosteroids, interleukin (IL)-3 and IL-6, in addition to EPO [15]. Although FL is the most active organ for erythropoiesis, little is known about how erythropoiesis is regulated in that tissue.

Here, in order to identify niche cells for erythropoiesis, we used flow cytometry based on surface molecule expression to separate cells in early FL into hepatoblasts (HBs), sinusoid endothelial cells (SECs) and hematopoietic cells (HCs), and then evaluated cytokine expression in each fraction.

2. Materials and methods

2.1. Animals

ICR and C57BL/6J mice were purchased from Nihon SLC (Hamamatsu, Japan) and Kyudo (Tosu, Japan), respectively. *Map2k4*$^{+/-}$ mice were provided by RIKEN BioResource Center (Tsukuba, Japan). Noon of the day of the plug was defined as 0.5 day post-coitum (dpc). Embryos at 12.5 and 14.5 dpc were dissected in PBS under a stereomicroscope. Animals were handled according to Guidelines for Laboratory Animals of Kyushu University.

* Corresponding author. Address: Division of Hematopoietic Stem Cells, Advanced Medical Initiatives, Department of Advanced Medical Initiatives, Kyushu University Faculty of Medical Sciences, Station for Collaborative Research1 4F, 3-1-1 Maidashi, Higashi-Ku, Fukuoka 812-8582, Japan. Fax: +81 92 642 6146.
E-mail address: ds-mons@yb3.so-net.ne.jp (D. Sugiyama).

0006-291X/$ - see front matter © 2011 Elsevier Inc. All rights reserved.
doi:10.1016/j.bbrc.2011.05.137

2.2. Flow cytometry

For hepatoblasts and sinusoid endothelial cells, fetal livers at 12.5 and 14.5 dpc were digested in 1 mg/mL collagenase (Washington Biochem Co., Freehold, New Jersey) in alpha-MEM containing 20% FBS, filtered through 40-μm nylon mesh, and washed once with PBS. Cells were stained with a FITC-conjugated anti-mouse Dlk-1 Ab (MBL, Nagoya, Japan), a PE-conjugated anti-mouse Lyve-1 Ab (MBL), an APC-conjugated anti-mouse CD31 Ab (Biolegend, San Diego, CA), a PE-Cy7-conjugated anti-mouse CD45 Ab (eBioscience, San Diego, CA), and a PE-Cy7-conjugated anti-mouse Ter119 Ab (eBioscience).

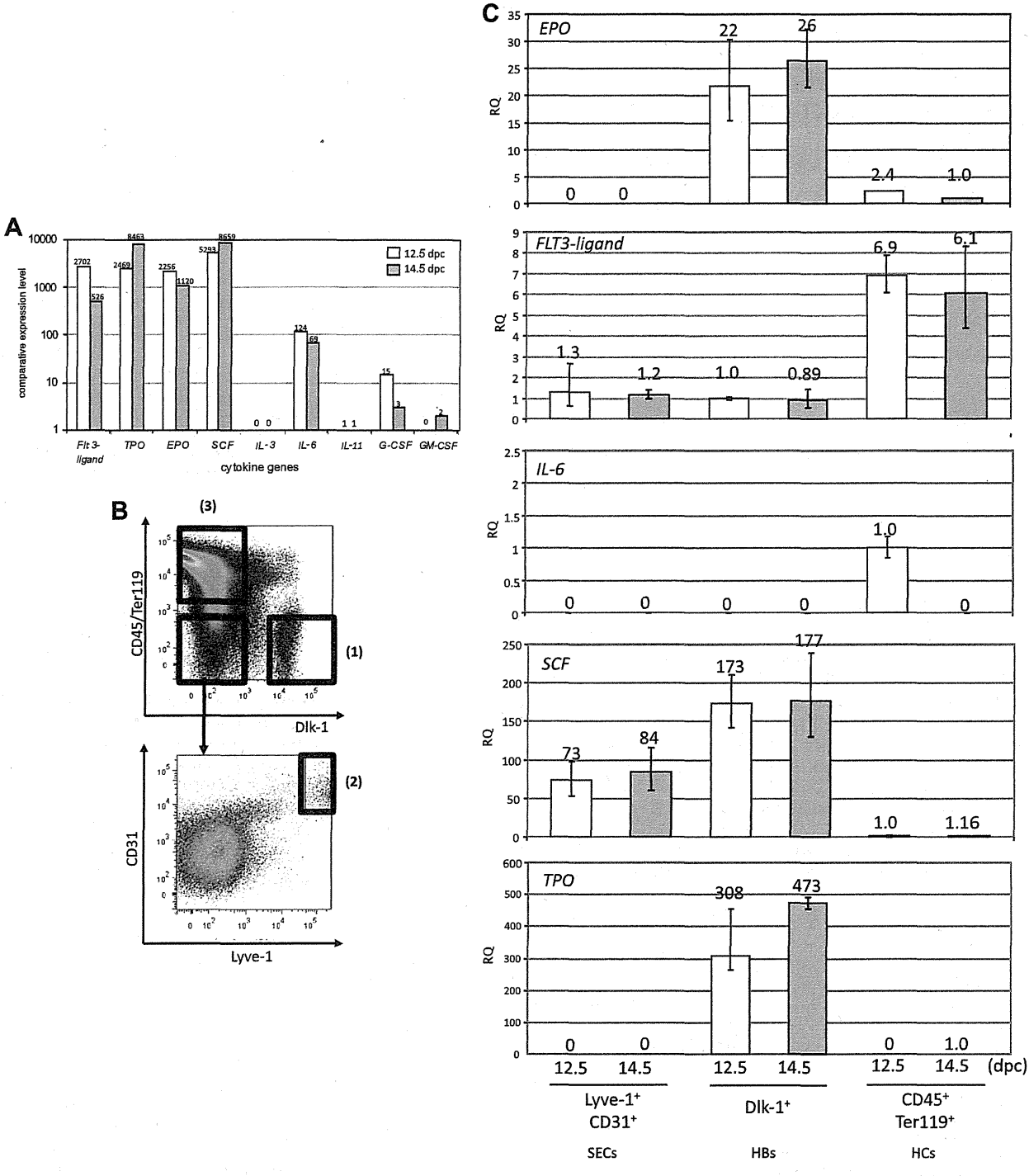

Fig. 1. Cytokine gene expression in fetal liver. (A) *FMS-like tyrosine kinase 3 ligand (Flt3l), thrombopoietin (TPO), eryrhropoietin (EPO), stem cell factor (SCF), interleukin-3 (IL-3), interleukin-6 (IL-6), interleukin-11 (IL-11), granulocyte-colony stimulating factor (G-CSF) and granulocyte/macrophage-colony stimulating factor (GM-CSF)* mRNAs were examined in FL samples at 12.5 and 14.5 dpc by real-time PCR. Note high expression of *Flt3l, TPO, EPO* and *IL-6* in FL. (B) A single cell suspension was obtained from FL at 12.5 dpc and expression of CD45/Ter119, Dlk-1, Lyve-1 and CD31 was analyzed by flow cytometry. (1) CD45−/Ter119−/Dlk-1+ defines HBs; (2) CD45−/Ter119−/Lyve-1+/CD31+ defines SECs; and (3) CD45+/Ter119+ defines HCs. (C) Expression of *Flt3l, TPO, EPO* and *IL-6* was examined by real-time PCR in HBs, SECs and HCs sorted by flow cytometry, according to gates defined in Fig. 1B. EPO and TPO expression was high in HBs at both 12.5 dpc and 14.5 dpc. SCF expression was higher in HBs than in SECs. Expression of *Flt3l* was high in HCs. Expression of *IL-6* was detected only in HCs.